

CNU-HEP-15-07, FERMILAB-PUB-15-508-T, EFI-15-36  
 MAN/HEP/2015/19, KCL-PH-TH/2015-49, LCTS/2015-37, CERN-PH-TH/2015-252

## CP Violation in Heavy MSSM Higgs Scenarios

M. Carena<sup>a,b,c</sup>, J. Ellis<sup>d,e</sup>, J. S. Lee<sup>f</sup>, A. Pilaftsis<sup>e,g</sup>, and C. E. M. Wagner<sup>b,c,h</sup>

<sup>a</sup>*Fermi National Accelerator Laboratory, P.O. Box 500, Batavia IL 60510, U.S.A.*

<sup>b</sup>*Enrico Fermi Institute, University of Chicago, Chicago, IL 60637, U.S.A.*

<sup>c</sup>*Kavli Institute for Cosmological Physics, University of Chicago, Chicago, IL 60637, U.S.A.*

<sup>d</sup>*Theoretical Particle Physics and Cosmology Group, Department of Physics,  
 King's College London, London WC2R 2LS, United Kingdom*

<sup>e</sup>*Theory Division, CERN, CH-1211 Geneva 23, Switzerland*

<sup>f</sup>*Department of Physics, Chonnam National University,  
 300 Yongbong-dong, Buk-gu, Gwangju, 500-757, Republic of Korea*

<sup>g</sup>*Consortium for Fundamental Physics, School of Physics and Astronomy  
 University of Manchester, Manchester M13 9PL, United Kingdom*

<sup>h</sup>*HEP Division, Argonne National Laboratory, 9700 Cass Ave., Argonne, IL 60439, USA*

### ABSTRACT

We introduce and explore new heavy Higgs scenarios in the Minimal Supersymmetric Standard Model (MSSM) with explicit CP violation, which have important phenomenological implications that may be testable at the LHC. For soft supersymmetry-breaking scales  $M_S$  above a few TeV and a charged Higgs boson mass  $M_{H^\pm}$  above a few hundred GeV, new physics effects including those from explicit CP violation decouple from the light Higgs boson sector. However, such effects can significantly alter the phenomenology of the heavy Higgs bosons while still being consistent with constraints from low-energy observables, for instance electric dipole moments. To consider scenarios with a charged Higgs boson much heavier than the Standard Model (SM) particles but much lighter than the supersymmetric particles, we revisit previous calculations of the MSSM Higgs sector. We compute the Higgs boson masses in the presence of CP violating phases, implementing improved matching and renormalization-group (RG) effects, as well as two-loop RG effects from the effective two-Higgs Doublet Model (2HDM) scale  $M_{H^\pm}$  to the scale  $M_S$ . We illustrate the possibility of non-decoupling CP-violating effects in the heavy Higgs sector using new benchmark scenarios named **CPX4LHC**.

PACS: 12.60.Jv, 13.20.He, 14.80.Cp

KEYWORDS: Higgs bosons; Supersymmetry; CP; LHC.

# 1 Introduction

Supersymmetry (SUSY) remains one of the best-motivated extensions of the Standard Model (SM), despite the current lack of evidence for supersymmetric partner particles at the LHC. In particular, the discovery of a light Higgs boson in Run I of the LHC, is in agreement with the predictions from SUSY. Supersymmetric theories provide a viable mechanism for stabilizing the electroweak vacuum [1] and require a restricted range for the mass of the lightest Higgs boson [2–4] that contains the measured value [5]. Moreover, minimal low-energy SUSY models with masses of the additional Higgs bosons and supersymmetric particles larger than the weak scale lead to values of the lightest Higgs couplings that are close to the SM ones [6], as suggested by current LHC experiments [7].

On the other hand, the non-discovery of SUSY in Run I of the LHC has disproved benchmark scenarios proposed previously [8], and motivates the consideration of new benchmarks that can be tested in future runs of the LHC. Specifically, it is plausible to consider the case that the common soft SUSY-breaking scale  $M_S$  is  $\gtrsim 2$  TeV, whereas the mass scale  $M_H$  of the heavy MSSM Higgs bosons, as determined by the charged Higgs boson mass  $M_{H^+}$ , could be somewhat lower, in the few to several hundred GeV range. In relation to this, we recall that future runs of the LHC at 13/14 TeV are expected to be sensitive to squarks and gluinos weighing  $\lesssim 3$  TeV, and heavy MSSM Higgs bosons weighing  $\lesssim 2$  TeV depending on the value of  $\tan\beta$ . Accordingly, in this paper we introduce and explore MSSM Higgs boson benchmark scenarios with  $100 \text{ GeV} \ll M_H \ll M_S \gtrsim 2 \text{ TeV}$ .

Our principal interest in new heavy Higgs boson benchmark scenarios is the possible manifestation of observable CP violation in the Higgs sector of the MSSM. It is well known [9–17] that such a possibility arises in the MSSM Higgs potential beyond the tree-level approximation, predominantly from CP phases in the soft SUSY-breaking trilinear couplings of stops and sbottoms, but also from CP phases in the gaugino masses. However, experimental upper limits on electric dipole moments (EDMs) severely constrain the size of such CP-violating parameters as predicted in the MSSM at one-, two- and higher loops [18]. In particular, in the absence of cancellations between these different contributions [19, 20] as occur along specific directions in the space of CP-odd phases [21, 22], the EDM constraints effectively preclude the observation of CP-violating effects in the couplings of the Higgs boson discovered at the LHC [23]. However, the observation of CP violation effects elsewhere, notably in the heavy MSSM Higgs sector [10, 11, 14] or  $B$ -meson decays [24, 25] is not excluded. These CP-violating effects have often been studied in the framework of the CPX scenarios proposed previously [8], but in light of the LHC Run-I limits on supersymmetric particle masses and the observed Higgs boson properties, the CPX benchmarks should be revisited.

With the above motivations in mind, in this paper we present new precision calculations of the MSSM Higgs spectrum in the presence of CP violation, which are suitable for scenarios in which the SUSY scale  $M_S$  is (far) beyond the TeV region. To this end, we solve the two-loop RGEs of the two-Higgs-doublet model (2HDM) in the range  $M_S > Q > M_H$ , as well as the two-loop SM RGEs in the range  $M_H > Q > m_t^{\text{pole}}$ , implementing full one-loop matching conditions at the relevant thresholds  $M_S$ ,  $M_H$  and  $m_t^{\text{pole}}$ . All the improvements considered

here are being implemented in a new version of the public code **CPsuperH** [26–28], namely **CPsuperH3.0** \*. The full description with all the detailed information about **CPsuperH3.0** will be presented in a future publication.

Section 2 of this paper reviews the conventions and notations of **CPsuperH** that we use for our analysis, as well as some basic formulae for the Higgs boson self-energies. Section 3 specifies the matching conditions and the RG running effects that we incorporate. In section 4 we present some numerical results for the Higgs spectra. In section 5 we introduce our new CP-violating benchmark scenarios (**CPX4LHC**) for the MSSM heavy Higgs sector, and present the results for the **CPX4LHC** benchmarks. Our conclusions are summarized in Section 6. The main text of the paper is accompanied by Appendices containing detailed formulae: Appendix A contains the relevant SM RGEs, Appendix B contains the one-loop 2HDM RGEs, Appendix C contains the two-loop 2HDM RGEs, and Appendix D summarizes the threshold corrections to quartic couplings at the scale  $M_S$ .

## 2 The CP-Violating MSSM Higgs Sector

In this section we review the computation of the Higgs boson self-energies and pole masses and record the basic expressions used in **CPsuperH3.0**, that underlie our present analysis. We follow the conventions and notations of **CPsuperH** [26–28], unless stated otherwise explicitly.

### 2.1 The Two-Higgs-Doublet Model (2HDM)

The tree-level 2HDM Higgs potential can be written as [11]:

$$\begin{aligned} \mathcal{L}_V = & \mu_1^2(\Phi_1^\dagger \Phi_1) + \mu_2^2(\Phi_2^\dagger \Phi_2) + m_{12}^2(\Phi_1^\dagger \Phi_2) + m_{12}^{*2}(\Phi_2^\dagger \Phi_1) + \lambda_1(\Phi_1^\dagger \Phi_1)^2 + \lambda_2(\Phi_2^\dagger \Phi_2)^2 \\ & + \lambda_3(\Phi_1^\dagger \Phi_1)(\Phi_2^\dagger \Phi_2) + \lambda_4(\Phi_1^\dagger \Phi_2)(\Phi_2^\dagger \Phi_1) + \lambda_5(\Phi_1^\dagger \Phi_2)^2 + \lambda_5^*(\Phi_2^\dagger \Phi_1)^2 \\ & + \lambda_6(\Phi_1^\dagger \Phi_1)(\Phi_1^\dagger \Phi_2) + \lambda_6^*(\Phi_1^\dagger \Phi_1)(\Phi_2^\dagger \Phi_1) + \lambda_7(\Phi_2^\dagger \Phi_2)(\Phi_1^\dagger \Phi_2) + \lambda_7^*(\Phi_2^\dagger \Phi_2)(\Phi_2^\dagger \Phi_1). \end{aligned} \quad (1)$$

The relations between these and the conventional MSSM parameters are

$$\begin{aligned} \mu_1^2 &= -m_1^2 - |\mu|^2, & \mu_2^2 &= -m_2^2 - |\mu|^2, & \lambda_1 &= \lambda_2 = -\frac{1}{8}(g^2 + g'^2), \\ \lambda_3 &= -\frac{1}{4}(g^2 - g'^2), & \lambda_4 &= \frac{1}{2}g^2, & \lambda_5 &= \lambda_6 = \lambda_7 = 0. \end{aligned} \quad (2)$$

The doublet Higgs fields may be decomposed as follows:

$$\Phi_1 = \begin{pmatrix} \phi_1^+ \\ \frac{1}{\sqrt{2}}(v_1 + \phi_1 + ia_1) \end{pmatrix}, \quad \Phi_2 = e^{i\xi} \begin{pmatrix} \phi_2^+ \\ \frac{1}{\sqrt{2}}(v_2 + \phi_2 + ia_2) \end{pmatrix}, \quad (3)$$

where the charged and neutral Goldstone bosons,  $G^\pm$  and  $G^0$ , are determined through the relations:

$$\begin{pmatrix} G^+ \\ H^+ \end{pmatrix} = \begin{pmatrix} c_\beta & s_\beta \\ -s_\beta & c_\beta \end{pmatrix} \begin{pmatrix} \phi_1^+ \\ \phi_2^+ \end{pmatrix}, \quad \begin{pmatrix} G^0 \\ a \end{pmatrix} = \begin{pmatrix} c_\beta & s_\beta \\ -s_\beta & c_\beta \end{pmatrix} \begin{pmatrix} a_1 \\ a_2 \end{pmatrix}, \quad (4)$$

---

\*For another tool to calculate CP-violating effects in the MSSM, see [29, 30].

with  $s_\beta \equiv \sin \beta$ ,  $c_\beta \equiv \cos \beta$  and  $\tan \beta = v_2/v_1$ .

To make contact with the notations used in [31], we make the following identifications:  $H_u = \Phi_2$  and  $H_d = \tilde{\Phi}_1 = i\tau_2\Phi_1^* = (\phi_1^{0*}, -\phi_1^-)^T$ . Moreover, the kinematic parameters as defined in [31] are related to ours as follows:

$$\begin{aligned} m_{11}^2 &\rightarrow -\mu_1^2, & m_{22}^2 &\rightarrow -\mu_2^2, & m_{12}^2 &\rightarrow +m_{12}^2, \\ \lambda_1 &\rightarrow -2\lambda_1, & \lambda_2 &\rightarrow -2\lambda_2, & \lambda_3 &\rightarrow -\lambda_3, & \lambda_4 &\rightarrow -\lambda_4, \\ \lambda_5 &\rightarrow -2\lambda_5, & \lambda_6 &\rightarrow -\lambda_6, & \lambda_7 &\rightarrow -\lambda_7, \\ g_2 &\rightarrow g, & g_1 &\rightarrow g'. & \cdots \end{aligned} \tag{5}$$

The one-loop 2HDM RGEs are given in Appendix B <sup>†</sup>, and the two-loop 2HDM RGEs are given in Refs. [32], [33] and Appendix C.

## 2.2 Charged Higgs Bosons

In the  $\{\phi_1^\pm, \phi_2^\pm\}$  basis, the RG-improved charged Higgs-boson self-energy matrix can be found in Eq. (2.6) of Ref. [16]:

$$\left(\hat{\Pi}^\pm\right)_{ij}(s) = -\left(\bar{\mathcal{M}}_\pm^2\right)_{ij} + (\xi_i^+ \xi_j^-)^{-1} \left(\Delta\Pi^\pm\right)_{ij}^{\tilde{f}}(s) + \left(\tilde{\Pi}^\pm\right)_{ij}^f(s). \tag{6}$$

The first term,  $\bar{\mathcal{M}}_\pm^2$ , is the two-loop Born-improved squared-mass matrix,

$$\bar{\mathcal{M}}_\pm^2 = \left(\frac{1}{2}\bar{\lambda}_4 v_1 v_2 + \Re \bar{m}_{12}^2\right) \begin{pmatrix} \tan \beta & -1 \\ -1 & \cot \beta \end{pmatrix}, \tag{7}$$

expressed in terms of relevant parameters such as the real part of the soft bilinear Higgs mixing,  $\Re \bar{m}_{12}^2$ , and the quartic coupling  $\bar{\lambda}_4$ . The bar on these parameters indicates the sum of the tree-level and of the one- and two-loop leading logarithmic contributions. When solving the 2HDM RGEs,  $\bar{\lambda}_4$  is to be estimated at the scale  $M_H$  where the heavy Higgs bosons decouple, and  $\Re \bar{m}_{12}^2$  is fixed when the charged-Higgs-boson pole mass is given as an input, as shown below.

The second term in (6) describes the threshold effects of the sfermions (top and bottom squarks) and is the product of two quantities: (i) the anomalous dimension factors  $\xi_i$

$$\xi_i = \exp \left[ - \int_{\ln M_H}^{\ln M_S} \gamma_i(t) dt \right], \tag{8}$$

defined in terms of the anomalous-dimensions of the external Higgs fields  $\gamma_i \equiv d \ln \Phi_i/dt$  (in this case the charged Higgs fields), and (ii) the scale-invariant one-loop threshold contribution from the top and bottom squarks

$$\left(\Delta\Pi^\pm\right)^{\tilde{f}} = \left(\frac{1}{2}\lambda_4^{(1)} v_1 v_2 + \Re m_{12}^{2(1)}\right) \begin{pmatrix} \tan \beta & -1 \\ -1 & \cot \beta \end{pmatrix} + \left(\tilde{\Pi}^\pm\right)^{\tilde{f}}. \tag{9}$$

---

<sup>†</sup>We note that the RGE running parameter used in Ref. [31] is related to ours by  $t \rightarrow 2t$ .

In the above, the SUSY-breaking scale  $M_S$  is used to decouple the heavy sfermions. Moreover, the superscript “(1)” in  $\lambda_4^{(1)}$  and  $\mathfrak{Rem}_{12}^{2(1)}$  indicates that these quantities contain the one-loop leading logarithmic contributions and they can be obtained from Eqs. (3.6) and (3.7) of [14] by choosing  $Q = M_S$ .

We note that the vacuum expectation values (VEVs)  $v_{1,2}$  of the Higgs doublets  $\Phi_{1,2}$ , and hence  $\tan \beta$ , evolve with the wave-function renormalization factors  $\xi_{1,2}$  of the corresponding neutral Higgs bosons:

$$v_i(M_S) = v_i(M_H)/\xi_i, \quad \tan \beta(M_S) = \tan \beta(M_H) \frac{\xi_1}{\xi_2}, \quad (10)$$

where  $\tan \beta(M_H)$  is the input value of  $\tan \beta$ , i.e. at the scale  $Q = M_H$ . Consequently, the SM VEV  $v$  is related to the Higgs VEVs  $v_{1,2}$  through:

$$v_1(M_H) = c_\beta(M_H) v(M_H), \quad v_2(M_H) = s_\beta(M_H) v(M_H). \quad (11)$$

The SM VEV  $v$  is fixed at the RG scale  $Q = m_t$ , by virtue of the relation:  $v(M_H) = v(m_t)/\xi_{\text{SM}}$ , where

$$\xi_{\text{SM}} = \exp \left[ - \int_{\ln m_t}^{\ln M_H} \gamma(t) dt \right]. \quad (12)$$

Here  $\gamma(t)$  is the anomalous dimension of the SM Higgs doublet, which is given in (A.12) in the one-loop approximation.

Finally, the last terms on the RHSs of (9) and (6), namely  $(\tilde{\Pi}^\pm)^{\tilde{f}/f}$  and  $(\tilde{\Pi}^\pm)^{f}$ , can be expressed as follows,

$$(\tilde{\Pi}^\pm)^{\tilde{f}/f} = (\Pi^\pm)^{\tilde{f}/f} + \begin{pmatrix} \frac{(T_{\phi_1})^{\tilde{f}/f}}{v_1} & i \frac{(T_a)^{\tilde{f}/f}}{v} \\ -i \frac{(T_a)^{\tilde{f}/f}}{v} & \frac{(T_{\phi_2})^{\tilde{f}/f}}{v_2} \end{pmatrix}, \quad (13)$$

with all quantities in the RHS of (13) computed in the  $\overline{\text{MS}}$  scheme. Explicit one-loop calculations yield

$$\begin{aligned} (\Pi^\pm)^{\tilde{f}} &= \Pi^{\pm(a)} + \Pi^{\pm(b)}, & (T_{\phi_{1,2}})^{\tilde{f}} &= T_{\phi_{1,2}}^{(d)}, & (T_{a_{1,2}})^{\tilde{f}} &= T_{a_{1,2}}^{(d)}, \\ (\Pi^\pm)^f &= \Pi^{\pm(c)}, & (T_{\phi_{1,2}})^f &= T_{\phi_{1,2}}^{(e)}, & (T_{a_{1,2}})^f &= 0, \end{aligned} \quad (14)$$

with  $T_a = T_{a_2}/c_\beta = -T_{a_1}/s_\beta$  and where  $\Pi^{\pm(a)}$ ,  $\Pi^{\pm(b)}$ ,  $\Pi^{\pm(c)}$ ,  $T_{\phi_{1,2}}^{(d)}$ ,  $T_{a_{1,2}}^{(d)}$ , and  $T_{\phi_{1,2}}^{(e)}$  are given by Eqs. (B.12), (B.13), (B.15), and (B.16) in [16]. The sfermionic contributions should be calculated at the scale  $M_S$ , whereas the fermionic contributions are evaluated at  $M_H$ .

In the  $\{G^\pm, H^\pm\}$  basis, the inverse-propagator matrix of the charged Higgs bosons is given by

$$\hat{\Delta}_\pm^{-1}(s) = s \mathbf{1}_{2 \times 2} + \begin{pmatrix} c_\beta & s_\beta \\ -s_\beta & c_\beta \end{pmatrix} \hat{\Pi}^\pm(s) \begin{pmatrix} c_\beta & -s_\beta \\ s_\beta & c_\beta \end{pmatrix}, \quad (15)$$

where we have defined

$$\left(\hat{\Pi}^\pm\right)_{ij}(s) = -\left(\bar{\mathcal{M}}_\pm^2\right)_{ij} + \left(\Delta\hat{\Pi}^\pm\right)_{ij}(s). \quad (16)$$

In (15), the  $\{22\}$  matrix element of the second term is given by

$$\begin{aligned} \left(\hat{\Pi}^\pm\right)_{11} s_\beta^2 - \left[\left(\hat{\Pi}^\pm\right)_{12} + \left(\hat{\Pi}^\pm\right)_{21}\right] s_\beta c_\beta + \left(\hat{\Pi}^\pm\right)_{22} c_\beta^2 \\ = -\left(\frac{1}{2}\bar{\lambda}_4 v^2 + \frac{\Re\bar{m}_{12}^2}{c_\beta s_\beta}\right) + \Delta\hat{\Pi}_{H^+H^-}, \end{aligned} \quad (17)$$

with

$$\Delta\hat{\Pi}_{H^+H^-} \equiv \left(\Delta\hat{\Pi}^\pm\right)_{11} s_\beta^2 - \left[\left(\Delta\hat{\Pi}^\pm\right)_{12} + \left(\Delta\hat{\Pi}^\pm\right)_{21}\right] s_\beta c_\beta + \left(\Delta\hat{\Pi}^\pm\right)_{22} c_\beta^2. \quad (18)$$

This yields the pole mass condition

$$\begin{aligned} \Re\left(\hat{\Delta}_\pm^{-1}\right)_{22}(s = M_{H^\pm}^2) \\ = M_{H^\pm}^2 - \left(\frac{1}{2}\bar{\lambda}_4 v^2 + \frac{\Re\bar{m}_{12}^2}{c_\beta s_\beta}\right) + \Re\Delta\hat{\Pi}_{H^+H^-}(s = M_{H^\pm}^2) = 0, \end{aligned} \quad (19)$$

which may be used to eliminate  $\Re\bar{m}_{12}^2$  in favor of the charged-Higgs boson pole mass  $M_{H^\pm}^2$ .

## 2.3 Neutral Higgs Bosons

In the  $\{\phi_1, \phi_2, a_1, a_2\}$  basis, Eq. (2.14) of [16] takes the form

$$\hat{\Pi}^N(s) = \begin{pmatrix} \hat{\Pi}^S(s) & \hat{\Pi}^{SP}(s) \\ \left(\hat{\Pi}^{SP}(s)\right)^T & \hat{\Pi}^P(s) \end{pmatrix}, \quad (20)$$

with

$$\begin{aligned} \left(\hat{\Pi}^S\right)_{ij}(s) &= -\left(\bar{\mathcal{M}}_S^2\right)_{ij} + (\xi_i \xi_j)^{-1} \left(\Delta\hat{\Pi}^S\right)_{ij}^{\tilde{f}}(s) + \left(\tilde{\Pi}^S\right)_{ij}^f(s), \\ \left(\hat{\Pi}^P\right)_{ij}(s) &= -\left(\bar{\mathcal{M}}_P^2\right)_{ij} + (\xi_i \xi_j)^{-1} \left(\Delta\hat{\Pi}^P\right)_{ij}^{\tilde{f}}(s) + \left(\tilde{\Pi}^P\right)_{ij}^f(s), \\ \left(\hat{\Pi}^{SP}\right)_{ij}(s) &= (\xi_i \xi_j)^{-1} \left(\tilde{\Pi}^{SP}\right)_{ij}^{\tilde{f}}(s) + \left(\tilde{\Pi}^{SP}\right)_{ij}^f(s). \end{aligned} \quad (21)$$

where, in analogy with Eq. (8),  $\xi_i$  are the corresponding anomalous dimension factors of the neutral Higgs fields.

The quantities  $\bar{\mathcal{M}}_S^2$  and  $\bar{\mathcal{M}}_P^2$  appearing here may be written in the forms

$$\begin{aligned} \bar{\mathcal{M}}_S^2 &= \Re\bar{m}_{12}^2 \begin{pmatrix} \tan\beta & -1 \\ -1 & \cot\beta \end{pmatrix} - v^2 \begin{pmatrix} 2\bar{\lambda}_1 c_\beta^2 & \bar{\lambda}_{34} c_\beta s_\beta \\ \bar{\lambda}_{34} c_\beta s_\beta & 2\bar{\lambda}_2 s_\beta^2 \end{pmatrix}, \\ \bar{\mathcal{M}}_P^2 &= \Re\bar{m}_{12}^2 \begin{pmatrix} \tan\beta & -1 \\ -1 & \cot\beta \end{pmatrix}, \end{aligned} \quad (22)$$

where  $\bar{\lambda}_1$ ,  $\bar{\lambda}_2$ , and  $\bar{\lambda}_{34} = \bar{\lambda}_3 + \bar{\lambda}_4$  are to be evaluated by solving the 2HDM RGEs at the scale  $M_H$ .

The quantities  $\Delta\Pi^S$  and  $\Delta\Pi^P$  may be written as

$$\begin{aligned} (\Delta\Pi^S)^{\tilde{f}} &= \Re m_{12}^{2(1)} \begin{pmatrix} t_\beta & -1 \\ -1 & 1/t_\beta \end{pmatrix} - v^2 \begin{pmatrix} 2\lambda_1^{(1)} c_\beta^2 & \lambda_{34}^{(1)} c_\beta s_\beta \\ \lambda_{34}^{(1)} c_\beta s_\beta & 2\lambda_2^{(1)} s_\beta^2 \end{pmatrix} + (\tilde{\Pi}^S)^{\tilde{f}}, \\ (\Delta\Pi^P)^{\tilde{f}} &= \Re m_{12}^{2(1)} \begin{pmatrix} t_\beta & -1 \\ -1 & 1/t_\beta \end{pmatrix} + (\tilde{\Pi}^P)^{\tilde{f}}, \end{aligned} \quad (23)$$

where  $\lambda_{1,2,34}^{(1)}$  and  $\Re m_{12}^{2(1)}$  can be obtained from Eqs. (3.3), (3.4), (3.5), (3.6) and (3.7) of [14] by choosing  $Q = M_S$ .

The quantities  $\tilde{\Pi}^{S,P,SP}$  are given in the  $\overline{\text{MS}}$  scheme by Eq. (2.11) of [16]:

$$\begin{aligned} \tilde{\Pi}^S &= \Pi^S + \begin{pmatrix} \frac{T_{\phi_1}}{v_1} & 0 \\ 0 & \frac{T_{\phi_2}}{v_2} \end{pmatrix}, \\ \tilde{\Pi}^{SP} &= \Pi^{SP} + \frac{T_a}{v} \begin{pmatrix} 0 & +1 \\ -1 & 0 \end{pmatrix}, \\ \tilde{\Pi}^P &= \Pi^P + \begin{pmatrix} \frac{T_{\phi_1}}{v_1} & 0 \\ 0 & \frac{T_{\phi_2}}{v_2} \end{pmatrix}. \end{aligned} \quad (24)$$

Here,  $(\Pi^S)^{\tilde{f}}$  and  $(\Pi^S)^f$  are given by

$$(\Pi^S)^{\tilde{f}} = \Pi^{S,(a)} + \Pi^{S,(b)}, \quad (\Pi^S)^f = \Pi^{S,(c)}, \quad (25)$$

which are specified in Eqs. (B.5), (B.6), and (B.14) of [16]. In addition,  $(\Pi^P)^{\tilde{f}}$  and  $(\Pi^P)^f$  are given by

$$(\Pi^P)^{\tilde{f}} = \Pi^{P,(a)} + \Pi^{P,(b)}, \quad (\Pi^P)^f = \Pi^{P,(c)}, \quad (26)$$

which can be obtained from Eqs. (B.5), (B.6) by replacing  $\phi_i \rightarrow a_i$  and from Eq. (B.14) of [16]. Moreover, the CP-violating self-energies  $(\Pi^{SP})^{\tilde{f}}$  and  $(\Pi^{SP})^f$  may be expressed as

$$(\Pi^{SP})^{\tilde{f}} = \Pi^{SP,(a)}, \quad (\Pi^{SP})^f = 0. \quad (27)$$

The non-zero self-energy  $\Pi^{SP,(a)}$  is given by Eq. (B.11) of [16].

Finally, the inverse propagator matrix of the neutral Higgs bosons in the  $\{\phi_1, \phi_2, a, G^0\}$  basis is given by

$$\hat{\Delta}_N^{-1}(s) = s \mathbf{1}_{4 \times 4} + \begin{pmatrix} 1 & 0 & 0 & 0 \\ 0 & 1 & 0 & 0 \\ 0 & 0 & -s_\beta & c_\beta \\ 0 & 0 & c_\beta & s_\beta \end{pmatrix} \hat{\Pi}^N(s) \begin{pmatrix} 1 & 0 & 0 & 0 \\ 0 & 1 & 0 & 0 \\ 0 & 0 & -s_\beta & c_\beta \\ 0 & 0 & c_\beta & s_\beta \end{pmatrix}, \quad (28)$$

and the physical masses can be obtained from the pole-mass conditions. We should reiterate here that the parameter  $\tan \beta$  is defined at  $s = 0$ . In this kinematic limit, the Goldstone boson  $G^0$  decouples from the  $4 \times 4$  propagator matrix, independently of the presence of explicit CP violation in the theory [9], as a consequence of the Goldstone theorem.

### 3 Matching Conditions and RG Running Effects

Here we detail the  $\overline{\text{MS}}$  renormalization group approach that we follow for the computation of the masses and mixings of the neutral and charged Higgs bosons in the CP-violation case. In particular, we state explicitly our matching conditions at the relevant threshold scales. Given these matching conditions, we compute the RG running effects to the relevant gauge, Yukawa and quartic couplings between the different threshold scales.

To start with, we define the SUSY-breaking scale  $M_S$  by

$$M_S^2 \equiv \max \left( M_{Q_3}^2 + m_t^2, M_{U_3}^2 + m_t^2, M_{D_3}^2 + m_b^2, M_{L_3}^2 + m_\tau^2, M_{E_3}^2 + m_\tau^2 \right), \quad (29)$$

which acts as the SUSY threshold scale. For the purposes of this study, we ignore possible hierarchies between the third-generation sfermions, by assuming they are small as compared to the other two hierarchical scales: (i) the heavy Higgs-sector scale  $M_H \equiv M_{H^+}$ ; (ii) the top-quark mass  $m_t$ .

The matching conditions for the quartic and Yukawa couplings at the threshold  $M_S$  are as follows:

$$\begin{aligned} \bar{\lambda}_1 = \bar{\lambda}_2 &= -\frac{1}{8} (g^2 + g'^2), \quad \bar{\lambda}_3 = -\frac{1}{4} (g^2 - g'^2), \quad \bar{\lambda}_4 = \frac{1}{2} g^2; \\ h_t^{\text{MSSM}} &= \frac{h_t^{\text{2HDM}}}{1 + \delta_t + \cot \beta \Delta_t}, \\ h_b^{\text{MSSM}} &= \frac{h_b^{\text{2HDM}}}{1 + \delta_b + \tan \beta \Delta_b}, \\ h_\tau^{\text{MSSM}} &= \frac{h_\tau^{\text{2HDM}}}{1 + \tan \beta \Delta_\tau}, \end{aligned} \quad (30)$$

where  $\Delta_f = \Delta h_f / h_f^{\text{MSSM}}$ ,  $\delta_f = \delta h_f / h_f^{\text{MSSM}}$ , and  $\Delta h_f$  and  $\delta h_f$  are the supersymmetric threshold corrections to the third generation Yukawa couplings [14, 34]. The difference between  $\delta h_f$  and  $\Delta h_f$  is that  $\delta h_f$  is a radiative correction to the supersymmetric  $h_f^{\text{MSSM}}$  coupling of up-quarks, down-quarks and leptons. The coupling  $\Delta h_f$ , instead, is a loop-induced coupling of the fermions to the Higgs doublet to which they do not couple in the supersymmetric limit. Therefore, below the scale  $M_S$  the theory becomes a general 2HDM, with up-quarks coupled to  $\Phi_2$  and down-quarks and leptons coupled to  $\Phi_1$ , with couplings given by  $h_f^{\text{MSSM}}(1 + \delta_f)$ , respectively, but with additional loop-induced couplings  $\Delta h_f$  to the other Higgs doublet. The couplings  $h_f^{\text{2HDM}}$  are the combinations of these Yukawa couplings related to the running fermion masses in the same way as in a Type-II 2HDM. Notice that in the present approach,

we treat the loop-induced couplings  $\Delta h_f$  as small departures from a Type-II 2HDM. Hence, we are working in a Type-II approximation to a general 2HDM.

The RGEs for the 2HDM used for  $M_S > Q > M_H$  are described in Appendices B and C. At the heavy Higgs threshold  $M_H \equiv M_{H^\pm}$ , the following matching conditions are employed:

$$\begin{aligned}\lambda &= \frac{\left(M_{H_1}^{\text{EP}}\right)^2}{v^2} - \frac{1}{16}\kappa(g^2 + g'^2)^2 s_{4\beta}^2, \\ h_t^{\text{2HDM}} &= \frac{y_t}{s_\beta}, \quad h_b^{\text{2HDM}} = \frac{y_b}{c_\beta}, \quad h_\tau^{\text{2HDM}} = \frac{y_\tau}{c_\beta},\end{aligned}\quad (31)$$

where  $M_{H_1}^{\text{EP}}$  denotes the effective potential mass of the lightest neutral Higgs boson calculated in the limit of zero external momentum  $s = 0$ . In the above, we have ignored the small effects due to scheme conversion from dimensional regularization to dimensional reduction [35]. In practice, while evaluating the evolution of the gauge, Yukawa and quartic couplings, at  $M_H < Q < M_S$ , we have assumed an effective Type-II 2HDM, in which the Yukawa couplings are given by  $h_f^{\text{2HDM}}$  with the matching condition, Eq. (31) given at the scale  $M_H$ . As already mentioned above, this amounts to an approximate treatment of the loop-induced  $\Delta h_f$  effects on the computation of the Higgs boson masses and mixing angles.

At scales below the heavy Higgs scale  $M_H$ , the only physical degrees of freedom are the SM ones. The RGEs for the SM used for  $Q < M_H$  are described in Appendix A. We define the SM Higgs potential as

$$V(\Phi) = -\frac{m^2}{2}|\Phi|^2 + \frac{\lambda}{2}|\Phi|^4,$$

with  $\Phi = (0, (v + h)/\sqrt{2})^T$  and  $\lambda = m^2/v^2$ . Note that the quartic coupling of  $\Phi$  is defined with a factor (-2) difference compared to the quartic couplings of  $\Phi_{1,2}$  in Eq. (1). In order to compare with the experimental results, it is important to define the SM boundary conditions for the gauge, Yukawa and quartic couplings. In our work we use [36]

$$\begin{aligned}y_t &= 0.93697 + 0.00550 \left( \frac{m_t^{\text{pole}}}{\text{GeV}} - 173.35 \right) - 0.00042 \frac{\alpha_s(M_Z) - 0.1184}{0.0007}, \\ g_s &= 1.1666 + 0.00314 \frac{\alpha_s(M_Z) - 0.1184}{0.0007} - 0.00046 \left( \frac{m_t^{\text{pole}}}{\text{GeV}} - 173.35 \right), \\ g' &= 0.3587, \quad g = 0.6483, \quad y_b = 0.0156, \quad y_\tau = 0.0100.\end{aligned}\quad (32)$$

The pole mass-squared of the lightest Higgs boson is then given by [35]:

$$\begin{aligned}(M_{H_1}^{\text{pole}})^2 &= \lambda(m_t^{\text{pole}}) v^2(m_t^{\text{pole}}) \\ &+ \kappa \left\{ 3y_t^2(4\bar{m}_t^2 - m_h^2) B_0(m_h^2, \bar{m}_t^2, \bar{m}_t^2) - \frac{9}{2}\lambda m_h^2 \left[ 2 - \frac{\pi}{\sqrt{3}} - \log \frac{m_h^2}{Q_{\text{RG}}^2} \right] \right\}\end{aligned}$$

$$\begin{aligned}
& -\frac{v^2}{4} \left[ 3g^4 - 4\lambda g^2 + 4\lambda^2 \right] B_0(m_t^2, M_W^2, M_W^2) \\
& -\frac{v^2}{8} \left[ 3(g^2 + g'^2)^2 - 4\lambda(g^2 + g'^2) + 4\lambda^2 \right] B_0(m_t^2, M_Z^2, M_Z^2) \\
& + \frac{1}{2}g^4 \left[ g^2 - \lambda \left( \log \frac{M_W^2}{Q_{\text{RG}}^2} - 1 \right) \right] + \frac{1}{4}(g^2 + g'^2) \left[ (g^2 + g'^2) - \lambda \left( \log \frac{M_Z^2}{Q_{\text{RG}}^2} - 1 \right) \right] \Big\}, \tag{33}
\end{aligned}$$

where  $\overline{m}_t = y_t v / \sqrt{2}$  and  $m_h^2 = \lambda(m_t^{\text{pole}}) v^2(m_t^{\text{pole}})$ . We take the renormalization group scale  $Q_{\text{RG}} = m_t^{\text{pole}}$ , and the function  $B_0$  used in (33) is defined in [16].

## 4 Numerical Results for the MSSM Higgs Sector

We first illustrate the effects of the RG running in the range of scales  $Q > M_H$  using a specific scenario with universal SUSY parameters fixed to be 1 TeV:

$$\mu = M_{1,2,3} = M_{\tilde{Q}_3, \tilde{U}_3, \tilde{D}_3, \tilde{L}_3, \tilde{E}_3} = A_{t,b,\tau} = 1 \text{ TeV}, \quad \rho_{\tilde{Q}, \tilde{U}, \tilde{D}, \tilde{L}, \tilde{E}} = 1, \tag{34}$$

where  $\rho_{\tilde{Q}} = M_{\tilde{Q}_{1,2}}/M_{\tilde{Q}_3}$ ,  $\rho_{\tilde{U}} = M_{\tilde{U}_{1,2}}/M_{\tilde{U}_3}$ , etc, and we have assumed no hierarchy between the three generations of sfermion masses.

Figure 1 illustrates with black lines the one-loop running of the 2HDM quartic couplings up to  $Q = 10^6$  GeV in the above scenario, Eq. (34), and compares them with the running of the corresponding combinations of electroweak gauge couplings (red lines). Since there is a single SUSY-breaking scale of 1 TeV and hence a single threshold, the couplings are matched at this scale, and the red and black lines diverge as  $Q$  decreases from  $M_S = 1$  TeV to  $M_H = M_{H^\pm} = 300$  GeV. Above  $M_S$  the RG evolution of the quartic couplings (black lines) are the same as those of the corresponding combinations of electroweak gauge couplings (red lines), i.e., the red and black lines lie on top of each other. This provides a non-trivial consistency check for the correctness of our results. In the same context, it is important to comment that, for values of  $\rho > 1$ , with  $\rho \equiv \max(\rho_{\tilde{Q}, \tilde{U}, \tilde{D}, \tilde{L}, \tilde{E}})$ , the proper matching conditions should be imposed at the highest soft SUSY-breaking scale  $M'_S = \rho M_S$ , rather than  $M_S$ . However, provided  $\rho$  is of order one, choosing  $M_S$  instead of  $M'_S$  as the matching scale produces no relevant differences in the computations of the Higgs-boson masses and mixing angles.

Next, we compare some results of **CPsuperH3.0** with the corresponding results of **CPsuperH2.3** in the MHMAX scenario [38, 39], where  $X_t = \sqrt{6}M_S$  and  $\mu = 200$  GeV. In order to isolate the effects of the running in the range  $M_H < Q < M_S$ , where the effective 2HDM description is valid, we consider examples with  $M_{H^\pm} \simeq m_t^{\text{pole}}$ . Figure 2 compares calculations of the lightest Higgs mass  $M_{H_1}$ , and Figure 3 shows results for the two heavier neutral Higgs bosons  $H_{1,2}$ , for  $M_{H^\pm} = 180$  GeV. In order to isolate the effects of the resummation of logarithms associated with the RG effects, we modified **CPsuperH2.3**, setting  $m_t(m_t^{\text{pole}}) = 162.88$  GeV as obtained using Eq. (32), instead of the value obtained from the one-loop relation between the pole and running masses:  $m_t(m_t^{\text{pole}}) =$

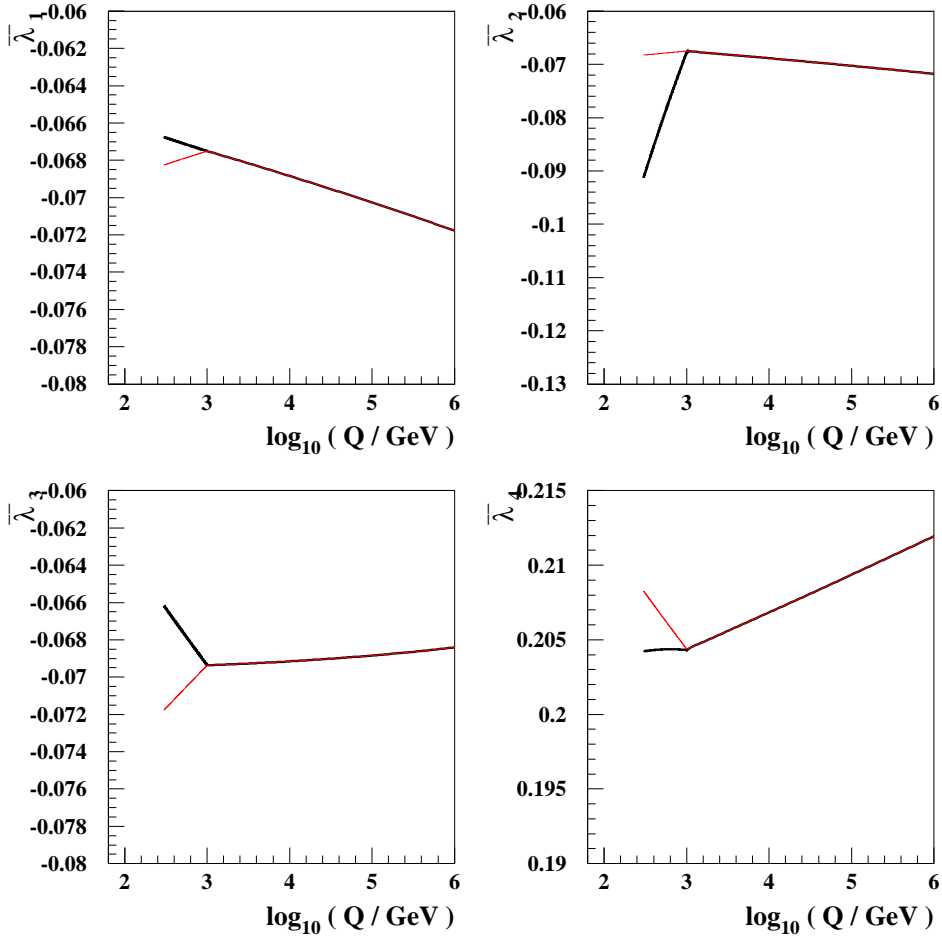


Figure 1: The black lines show the one-loop running of the 2HDM quartic couplings for  $Q < 10^6$  GeV, assuming  $M_{H^\pm} = 300$  GeV and  $\tan \beta = 5$ . The thin red lines show the running of  $-(g^2 + g'^2)/8$ ,  $-(g^2 - g'^2)/4$ , and  $g^2/2$  in the panels for  $\bar{\lambda}_{1,2}$ ,  $\bar{\lambda}_3$ , and  $\bar{\lambda}_4$ , respectively.

$m_t^{\text{pole}}/(1 + 4\alpha_s(m_t^{\text{pole}})/(3\pi)) \simeq 165.5$  GeV, that was the standard value in **CPsuperH2.3**. The lower value of the running top quark mass we use is based on higher-order loop corrections to the relation between the pole and running masses [36], [37] and, as stressed before, it is used as the standard value for **CPsuperH3.0**.

From Fig. 2 we see that in the MHMAX scenario, the mass of the lightest Higgs boson calculated using **CPsuperH3.0** is  $\sim 1$  GeV smaller than that obtained using **CPsuperH2.3** for  $M_S = M_{\tilde{Q}_3} = M_{\tilde{U}_3} = M_{\tilde{D}_3} = M_{\tilde{L}_3} = M_{\tilde{E}_3} = 1$  TeV <sup>‡</sup>. This  $\sim 1$  GeV difference may be attributed to the use of  $h_t^{\text{2HDM}}$  in **CPsuperH3.0** in the running to low energies. Namely, whereas in **CPsuperH2.3** the top Yukawa coupling appearing in  $\lambda_2^{(1),(2)}$  given by Eqs. (3.4) and (3.10) of Ref. [14] includes the threshold corrections, we have not included these corrections in **CPsuperH3.0**. These Yukawa thresholds are still included in the relevant computation

<sup>‡</sup>Here we ignore the small difference of  $M_S$  from that defined in Eq. (29), but this difference is taken into account in all the numerical results presented in this work.

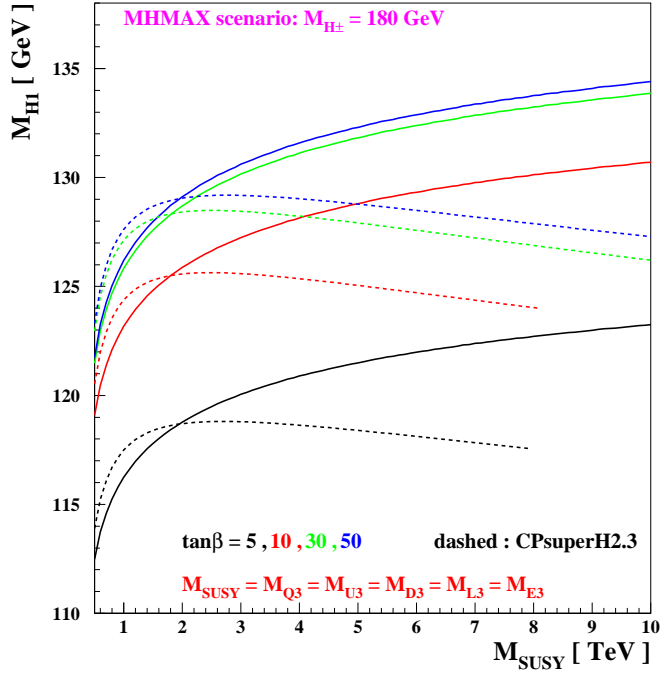


Figure 2: The lightest Higgs mass calculated in the MHMAX scenario using CPsuperH3.0 (solid lines) and CPsuperH2.3 (dashed lines) as functions of  $M_S = M_{Q3} = M_{U3} = M_{D3} = M_{L3} = M_{E3}$  for  $M_{H^\pm} = 180$  GeV,  $\mu = 200$  GeV and various values of  $\tan\beta$ .

of the threshold corrections to the quartic couplings, which lead to the asymmetry between positive and negative values of  $X_t = A_t - \mu^*/\tan\beta$  in the CP-conserving limit of the theory. This small difference between the CPsuperH3.0 and CPsuperH2.3 is rapidly compensated by RG effects and, as expected, the mass difference changes sign when  $M_S \sim 2$  TeV, and the new calculation of  $M_{H_1}$  is larger than the old one by  $\sim 5$  GeV when  $M_S \sim 8$  TeV, the difference being only weakly dependent on  $\tan\beta$ . We do not show results for CPsuperH2.3 at  $\tan\beta = 5$  and 10 and  $M_S > 8$  TeV, since this program becomes unstable for that region of parameters.

Figure 3 shows corresponding comparisons of the masses of the two heavier neutral Higgs bosons  $M_{H_{2,3}}$  for the same parameter values. We see that the differences are very small for  $\tan\beta = 5$  and 10, but increase for larger  $\tan\beta$  and larger  $M_S$ , reaching  $\sim 4$  GeV for  $\tan\beta = 50$  and  $M_S = 10$  TeV.

Figure 4 shows another comparison of calculations of  $M_{H_1}$  made using CPsuperH3.0 (solid lines) and CPsuperH2.3 (dashed lines), this time as a function of  $X_t/M_S$  for  $M_S = 1$  TeV (black lines), 2 TeV (red lines) and 4 TeV (blue lines). These calculations were made assuming  $M_{H^\pm} = 180$  GeV,  $\mu = M_2 = 2M_1 = 200$  GeV and  $\tan\beta = 20$ . We see that the differences in  $M_{H_1}$  are again small, i.e.,  $\lesssim 1$  GeV, for most values of  $X_t/M_S$ , though rising to  $\sim 2$  GeV for  $X_t/M_S \sim -2$ . The results of CPsuperH3.0 are in agreement with those obtained in Ref. [33]. Figure 5 compares calculations of  $M_{H_1}$  made within CPsuperH3.0 using the two-loop 2HDM RGEs (solid lines) and the one-loop 2HDM RGEs (dashed lines),

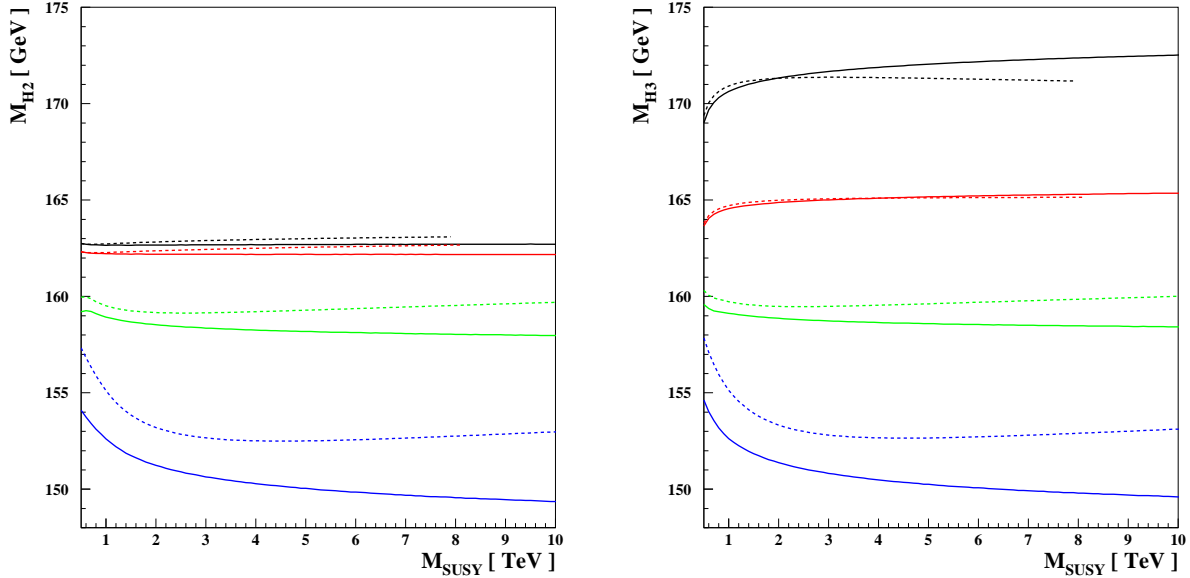


Figure 3: The two heavier neutral Higgs masses  $M_{H_{2,3}}$  calculated in the MHMAX scenario using CPsuperH3.0 (solid lines) and CPsuperH2.3 (dashed lines), for the same parameter choices as in Figure 2.

again as a function of  $X_t/M_S$  for  $M_S = 1$  TeV (black lines), 2 TeV (red lines) and 4 TeV (blue lines). We see that the full two-loop results are generally smaller than those in the one-loop approximation by  $< 1$  GeV, providing an encouraging estimate of their reliability.

Figure 6 shows some results from CPsuperH3.0 for some larger values of  $M_S$  and  $M_H = M_{H^\pm}$  where CPsuperH2.3 would have been inapplicable. The left panel shows  $M_{H_1}$  for  $M_{H^\pm} = M_S \leq 100$  TeV for two cases,  $\tan\beta = 4$  and  $X_t/M_S = \sqrt{6}$  (black line) and  $\tan\beta = 20$  and  $X_t/M_S = 0$  (red line) both for the case  $\mu = M_2 = 2M_1 = 200$  GeV considered in Figure 4. There is no 2HDM running effects in these plots, only the effects of SM running up to the common new physics threshold. Even allowing for an uncertainty of about 3 GeV in these calculations, values of  $M_S = M_{H^\pm} > 15$  TeV lead to values of the lightest Higgs mass  $M_{H_1}$  that are incompatible with the measured values at the LHC, so the extension of the  $M_S$  axis to 100 TeV is largely for illustrative purposes.

The right panel of Figure 6 shows some other results for larger values of  $M_{H^\pm}$  over the full range  $[m_t, M_S]$  for  $M_S = 1, 2$  and 4 TeV (black, red and blue lines, respectively) in the same two cases  $X_t/M_S = \sqrt{6}$ ,  $\tan\beta = 4$  and  $X_t/M_S = 0$ ,  $\tan\beta = 20$ , considered previously, again with  $\mu = M_2 = 2M_1 = 200$  GeV. For these values of  $\tan\beta$ , the measured values of the Higgs mass is consistent with  $M_S = 4$  TeV in the  $X_t/M_S = \sqrt{6}$ ,  $\tan\beta = 4$  case <sup>§</sup>.

<sup>§</sup>The results in the left and right panes of Figure 6 should be compared to the ones in the lower-left frames of Figs. 1 and 2, and of Fig. 6 in Ref. [35]

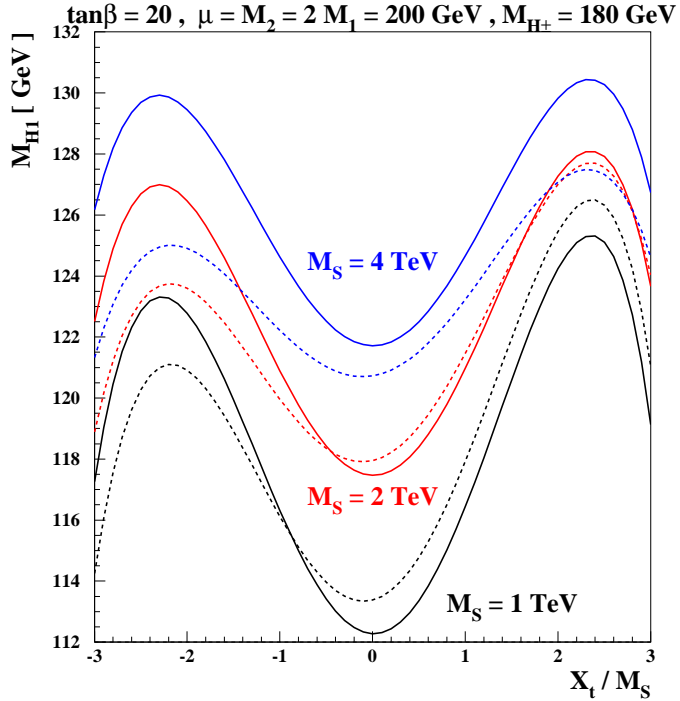


Figure 4: The lightest Higgs mass calculated as a function of  $X_t/M_S$  using CPsuperH3.0 (solid lines) and CPsuperH2.3 (dashed lines) for  $M_{H^\pm} = 180$  GeV,  $\mu = M_2 = 2M_1 = 200$  GeV and  $\tan\beta = 20$  for  $M_S = 1$  TeV (black lines), 2 TeV (red lines) and 4 TeV (blue lines).

## 5 CP-Violating Heavy Higgs Scenarios

We now consider various **CPX4LHC** benchmark scenarios for showcasing the effect of CP violation in the MSSM heavy Higgs sector and their possible signatures. We assume a common CP-violating phase  $\Phi_A = \arg(A_t) = \arg(A_b) = \arg(A_\tau)$ , set

$$|A_{t,b,\tau}| = \mu = 2M_S , \quad (35)$$

with  $M_2 = 2M_1 = 200$  GeV and  $M_3 = 2$  TeV, and vary  $\tan\beta$ ,  $M_{H^\pm}$ , and  $M_S$ . We do not include gaugino phases in this analysis, as they enter the Higgs sector only through the threshold corrections to the MSSM top-, bottom-, and tau-Yukawa couplings. Instead, we include the CP-conserving leading-log enhanced contributions due to gauginos to the self-energies  $\Pi^{\pm,S,P}$ . In our **CPX4LHC** scenarios, since we fix  $M_2 = 2M_1 = 200$  GeV and  $M_3 = 2$  TeV, and do not increase them as  $M_S$  increases, the gaugino phase effects are relatively insignificant.

We first present in Figure 7 results for  $M_{H_1}$  as a function of  $\Phi_A$  for the representative choices  $M_{H^\pm} = 500$  GeV,  $M_S = 1, 2, 5, 10$  TeV and  $\tan\beta = 5, 10, 30, 50$ . The changes in  $M_{H_1}$  as  $\Phi_A$  varies are small in general, namely  $\lesssim 3$  GeV for  $\tan\beta = 5$  and less for larger  $\tan\beta$ . Nevertheless, these variations are potentially significant, as there are parameter choices that

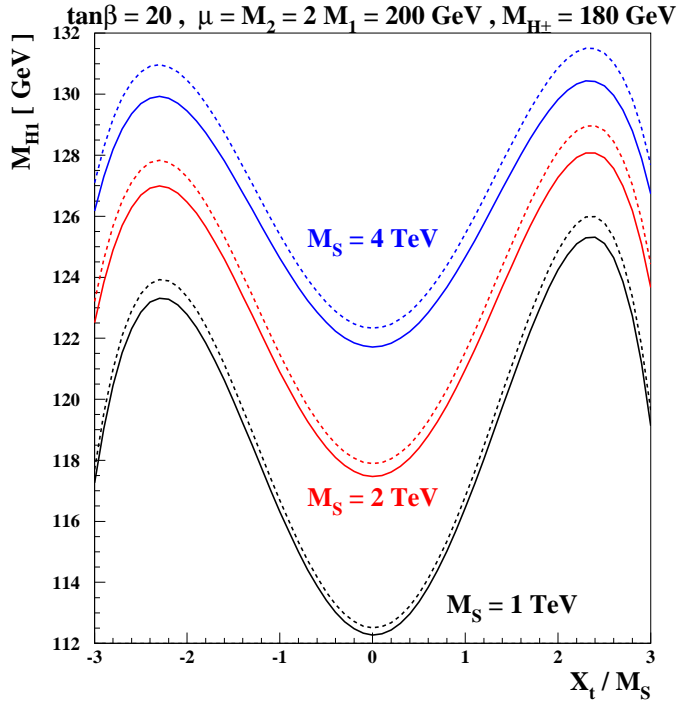


Figure 5: The lightest Higgs mass calculated as a function of  $X_t/M_S$  including (solid lines) and without including (dashed lines) the two-loop 2HDM contributions to the RGEs for  $M_{H^\pm} = 180$  GeV,  $\mu = M_2 = 2M_1 = 200$  GeV and  $\tan\beta = 20$  for  $M_S = 1$  TeV (black lines), 2 TeV (red lines) and 4 TeV (blue lines).

would be excluded (in the sense of yielding values of  $M_{H_1}$  more than 3 GeV different from the measured value) for  $\Phi_A = 0$  that would be allowed for  $\Phi_A \neq 0$ , e.g.,  $M_S = 5$  TeV and  $\tan\beta = 5$ . Conversely, there are cases where  $\Phi_A = 0$  would be allowed, but  $\Phi_A \neq 0$  would be disallowed, e.g.,  $M_S = 10$  TeV and  $\tan\beta = 10$ . The change in the lightest Higgs mass  $M_{H_1}$  at lower values of  $\tan\beta$  can be understood from the change in the modulus of  $X_t = A_t - \mu^*/\tan\beta$ , which governs the one-loop threshold corrections to the low-energy Higgs quartic coupling. It reaches a maximum when  $|X_t|/M_S \simeq 2.4$ , and becomes less significant as  $\tan\beta$  increases. In addition to this change, there are two-loop effects governed by the relative phase of  $A_t$  and  $M_3$ , which in the CP-conserving case tend to decrease (increase)  $M_{H_1}$  for negative (positive) values of  $A_t M_3^*$ , which explains why, for large values of  $\tan\beta$ , for which the variation of  $|X_t|$  is small, the maximum value of  $M_{H_1}$  occurs for  $\Phi(A_t) = 0$ .

Figure 8 displays the corresponding values of  $M_{H_3}$  (solid lines) and  $M_{H_2}$  (dashed lines) for  $M_{H^\pm} = 500$  GeV and the same values of  $M_S$  and  $\tan\beta$  as in Figure 7. We see that in general the mass difference  $M_{H_3} - M_{H_2}$  is minimized in the CP-conserving cases  $\Phi_A = 0, 180^\circ$ , where it is  $\lesssim 1$  GeV, and maximized when  $\Phi_A = \pm 90^\circ$ , where it may be  $\sim 3$  GeV. Thus, a measurement of the  $H_3 - H_2$  mass difference could be an indirect diagnostic tool indicative of CP violation, even if the latter is not directly observable.

We now consider predictions for two direct measures of CP violation in the Higgs mass

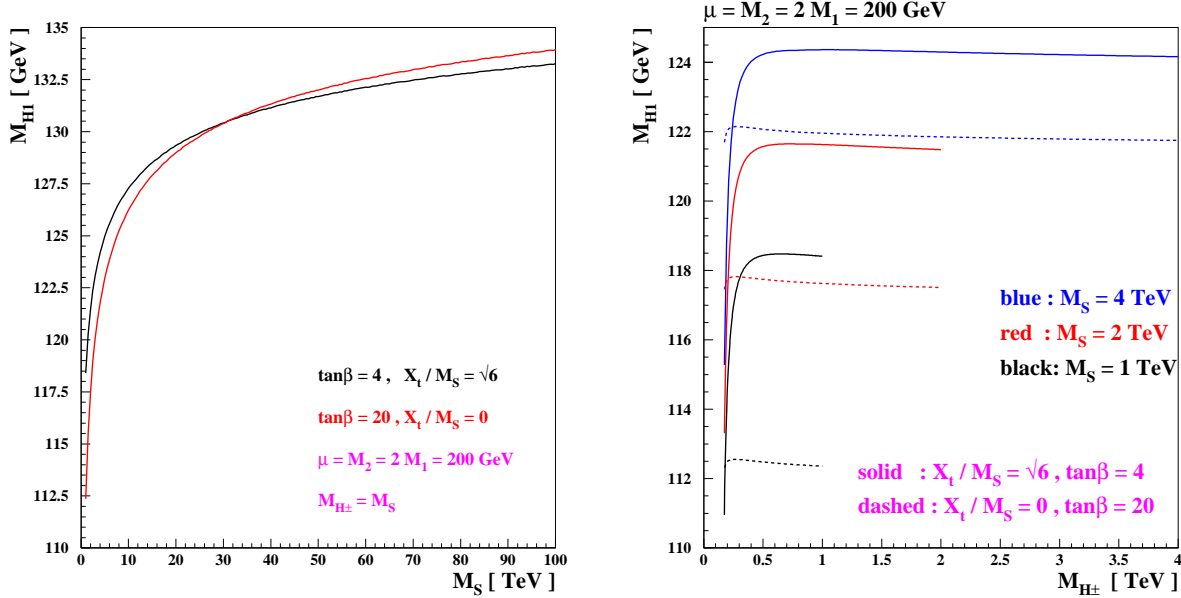


Figure 6: *Left panel:* Calculations of  $M_{H1}$  made using CPsuperH3.0 for  $M_{H^\pm} = M_S \leq 100$  TeV, assuming  $\tan\beta = 4$  and  $X_t/M_S = \sqrt{6}$  (black line) and  $\tan\beta = 20$  and  $X_t/M_S = 0$  (red line) both for the case  $\mu = M_2 = 2M_1 = 200$  GeV. *Right panel:* calculations of  $M_{H1}$  as a function of  $m_{H^\pm}$  made using CPsuperH3.0 over the range  $M_{H^\pm} \in [m_t, M_S]$  for  $M_S = 1, 2$  and 4 TeV (black, red and blue lines, respectively), also for the two cases  $X_t/M_S = \sqrt{6}$  and  $\tan\beta = 4$  (solid lines) and  $X_t/M_S = 0$  and  $\tan\beta = 20$  (dashed lines) and  $\mu = M_2 = 2M_1 = 200$  GeV. These results can be compared with those of [35].

eigenstates  $H_i$  (with  $i = 1, 2, 3$ ):

$$\langle \phi_1 a : H_i \rangle \equiv \frac{2O_{\phi_1 i} O_{ai}}{O_{\phi_1 i}^2 + O_{ai}^2}, \quad \langle \phi_2 a : H_i \rangle \equiv \frac{2O_{\phi_2 i} O_{ai}}{O_{\phi_2 i}^2 + O_{ai}^2}, \quad (36)$$

which characterize the mixtures between the CP-odd state  $a$  and the CP-even states  $\phi_{1,2}$ . For instance, such CP-violating expressions occur when studying CP violation in Higgs-boson decays to fermions [23, 40]. For a recent analysis of CP violation in the decays  $H_{1,2,3} \rightarrow \tau^+ \tau^-$ , see [41]. Figure 9 displays values of  $\langle \phi_1 a : H_1 \rangle$  for the lightest neutral mass eigenstate  $H_1$ , for the same scenarios  $M_{H^\pm} = 500$  GeV,  $M_S = 1, 2, 5, 10$  TeV and  $\tan\beta = 5, 10, 30$  and 50 discussed previously. We see that the values increase for smaller values of  $M_S$  and larger values of  $\tan\beta$ , and that values as large as  $\pm 0.22$  are possible for  $\tan\beta = 50$  and  $M_S = 1$  TeV. Even larger values would be possible for smaller values of  $M_{H^\pm}$  and  $M_S$ .

Fig 10 shows values of the other mixing coefficient  $\langle \phi_2 a : H_1 \rangle$  for  $H_1$  in the same set of CP-violating scenarios. This coefficient takes values  $\lesssim 0.007$  for  $M_{H^\pm} = 500$  GeV,  $M_S = 1$  TeV and  $\tan\beta = 5$ , decreasing for larger  $M_{H^\pm}$ ,  $M_S$  and  $\tan\beta$ .

Similar results for the second mass eigenstate  $H_2$  are shown in Figs. 11 and 12, and for the third mass eigenstate  $H_3$  in Figs. 13 and 14. We see here that the mixing quantities (36) can be *much larger* for the heavy mass eigenstates  $H_{2,3}$  than for the lightest mass eigenstate  $H_1$ , attaining unity for many of the values of  $M_S$  and  $\tan\beta$  studied. This suggests, *a priori*,

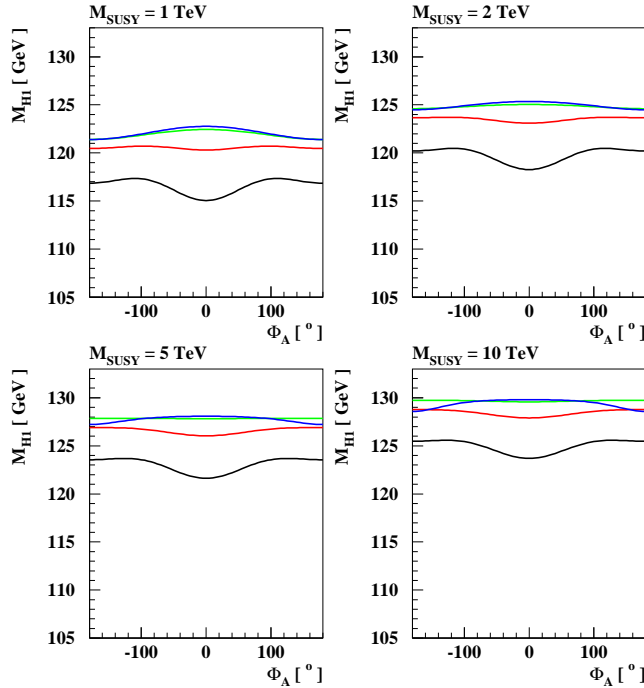


Figure 7: Values of  $M_{H_1}$  in CP-violating scenarios for  $M_{H^\pm} = 500$  GeV and  $M_S = 1$  TeV (upper left),  $M_S = 2$  TeV (upper right),  $M_S = 5$  TeV (lower left),  $M_S = 10$  TeV (lower right). The black, red, green and blue lines are for  $\tan\beta = 5, 10, 30$  and 50, respectively.

that the prospects for observing CP violation would be enhanced for the heavier Higgs mass eigenstates  $H_2$  and  $H_3$ .

These results illustrate the possible non-decoupling of CP-violating effects in the heavier neutral Higgs bosons  $H_{2,3}$  for large values of  $M_{H^\pm}$  and  $M_S$ , whereas the corresponding quantities for the lightest neutral Higgs mass eigenstate are expected to decouple. This is seen explicitly in Figs. 15, where we display the absolute values of  $\langle\phi_1 a : H_i\rangle$  (left) and  $\langle\phi_2 a : H_i\rangle$  (right) for  $M_S = 10$  TeV and  $\Phi_A = 10^\circ$  as functions of  $M_{H^\pm}$  for the same values of  $\tan\beta$  considered previously. The corresponding results for  $\Phi_A = 60^\circ$  are shown in Figure 16. In the case of  $H_1$ , we see that the mixing quantities  $\rightarrow 0$  at large  $M_{H^\pm}$ , as expected, whereas in general the corresponding coefficients for the heavy neutral Higgs mass eigenstates  $H_{2,3}$  do not vanish, and retain large values even for very large  $M_{H^\pm}$ . Thus, large CP-violating effects in the couplings of these states are a robust signature of the CP-violating scenarios discussed in this paper.

## 6 Conclusions

We present new MSSM scenarios with explicit CP violation that contain heavy Higgs bosons in the few to several hundred GeV range and are consistent with constraints from Run I of the LHC. The scenarios suggested here are similar in spirit to the CPX scenarios previously

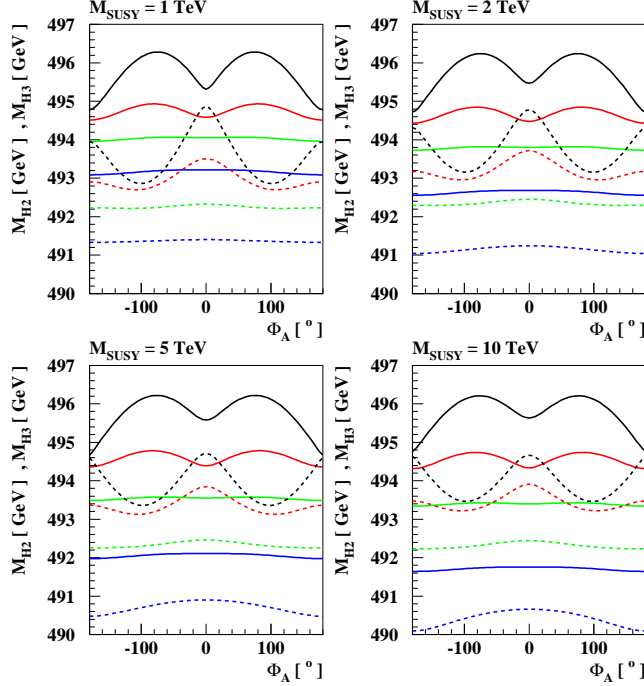


Figure 8: Values of  $M_{H_3}$  (solid lines) and  $M_{H_2}$  (dashed lines) in CP-violating scenarios for  $M_{H^\pm} = 500$  GeV and  $M_S = 1$  TeV (upper left),  $M_S = 2$  TeV (upper right),  $M_S = 5$  TeV (lower left),  $M_S = 10$  TeV (lower right). The black, red, green and blue lines are for  $\tan\beta = 5, 10, 30$  and 50, respectively.

proposed, and have phenomenological implications that can be tested during Run II of the LHC. In light of this, we call them **CPX4LHC** benchmark scenarios.

In this work we explicitly demonstrate that, although CP violation and other new-physics effects decouple from the lightest Higgs boson sector for sufficiently large charged Higgs boson masses and soft SUSY-breaking scales  $M_S$ , they can still be significant in the MSSM heavy Higgs boson sector. Large masses of the supersymmetric particles also help to maintain agreement with limits on EDMs and other low-energy observables. We consider scenarios in which the charged Higgs bosons  $H^\pm$  and the two heavier neutral Higgs bosons  $H_{2,3}$  could be much lighter than all third generation supersymmetric scalar fermions, which are assumed to have masses  $M_S \gtrsim 2$  TeV. In light of this possibility, we have revisited previous calculations by considering improved matching and renormalization group (RG) effects, specifically including two-loop RG effects in the two-Higgs-doublet model (2HDM) that is effective between the heavy Higgs scale  $M_{H^\pm}$  and the SUSY scale  $M_S$ .

We compare our new results with those obtained with the previous code version **CPsuperH2.3**. We also discuss the specific **CPX4LHC** benchmark scenarios relevant for the analysis of Higgs physics at the LHC, with particular emphasis on the masses of the heavier neutral Higgs bosons  $H_{2,3}$  and on the CP-violating effects they may manifest. These offer interesting prospects for future runs of the LHC and future colliders.

All the improvements discussed in this study are being incorporated in a new version of the public code **CPsuperH**, called **CPsuperH3.0**. The numerical results presented here have

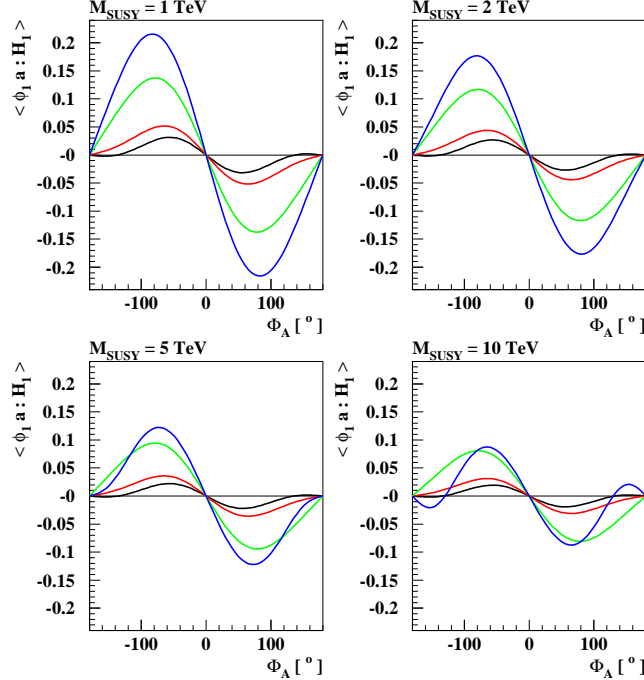


Figure 9: The CP mixing quantity  $\frac{2O_{\phi_1 1} O_{a1}}{O_{\phi_1 1}^2 + O_{a1}^2}$  for the lightest mass eigenstate  $H_1$  in scenarios with  $M_{H^\pm} = 500 \text{ GeV}$  and  $M_S = 1 \text{ TeV}$  (upper left),  $M_S = 2 \text{ TeV}$  (upper right),  $M_S = 5 \text{ TeV}$  (lower left),  $M_S = 10 \text{ TeV}$  (lower right). The black, red, green and blue lines are for  $\tan \beta = 5, 10, 30$  and  $50$ , respectively.

been obtained by means of a preliminary  $\beta$ -version of this code. The detailed features of CPsuperH3.0 will be fully described in an upcoming release note <sup>¶</sup>.

## Acknowledgements

Fermilab is operated by Fermi Research Alliance, LLC under Contract No. DE-AC02-07CH11359 with the U.S. Department of Energy, and University of Chicago is supported in part by U.S. Department of Energy grant number DE-FG02-13ER41958. The work of J.E. is supported in part by the London Centre for Terauniverse Studies (LCTS), using funding from the European Research Council via the Advanced Investigator Grant 267352, and in part by STFC (UK) via the research grant ST/L000326/1. The work of J.S.L. is supported by the National Research Foundation of Korea (NRF) grant (No. 2013R1A2A2A01015406). The work of A.P. is supported by the Lancaster-Manchester-Sheffield Consortium for Fundamental Physics under STFC grant ST/L000520/1. Work at ANL is supported in part by the U.S. Department of Energy under Contract No. DE-AC02-06CH11357. M.C. and C.W. thank for its hospitality the Aspen Center for Physics, which is supported by the National Science Foundation under Grant No. PHYS-1066293.

<sup>¶</sup>The current  $\beta$ -version is available upon request to J. S. Lee.

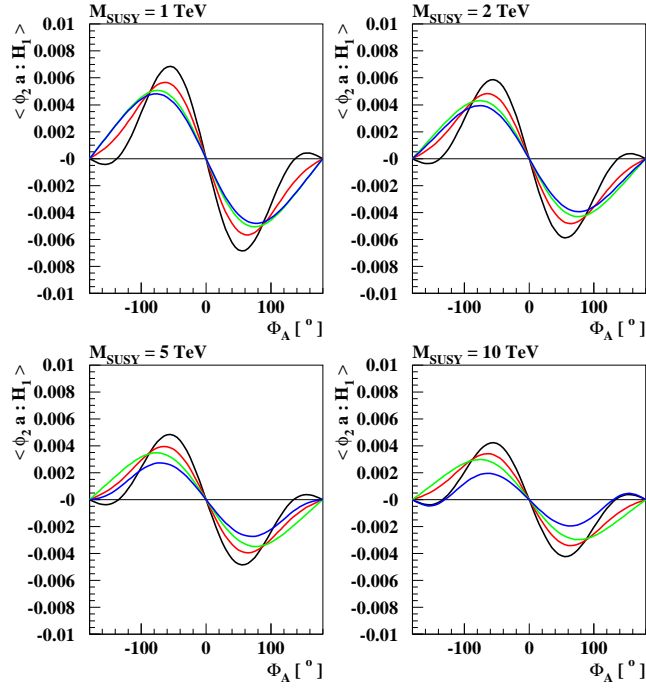


Figure 10: As in Figure 9, but showing the CP mixing quantity  $\frac{2O_{\phi_21}O_{a1}}{O_{\phi_21}^2+O_{a1}^2}$  for the lightest mass eigenstate  $H_1$ .

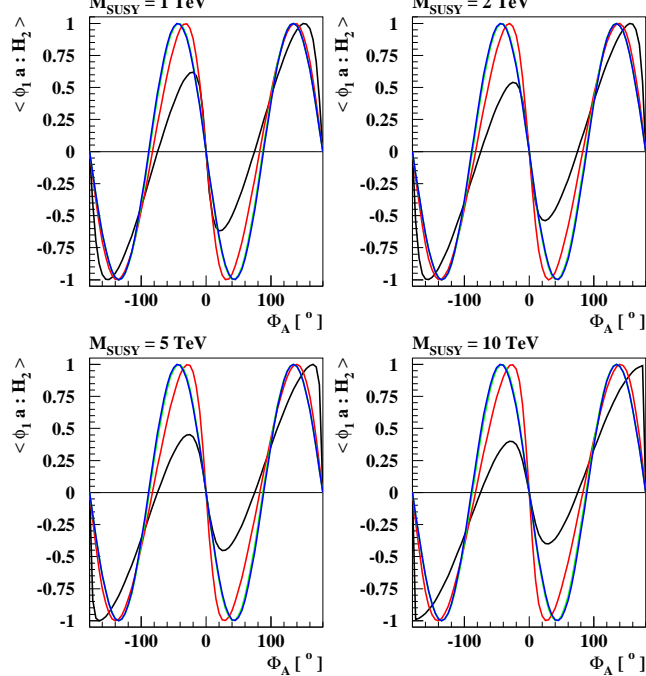


Figure 11: As in Figure 9, but showing the CP mixing quantity  $\frac{2O_{\phi_12}O_{a2}}{O_{\phi_12}^2+O_{a2}^2}$  for the second mass eigenstate  $H_2$ .

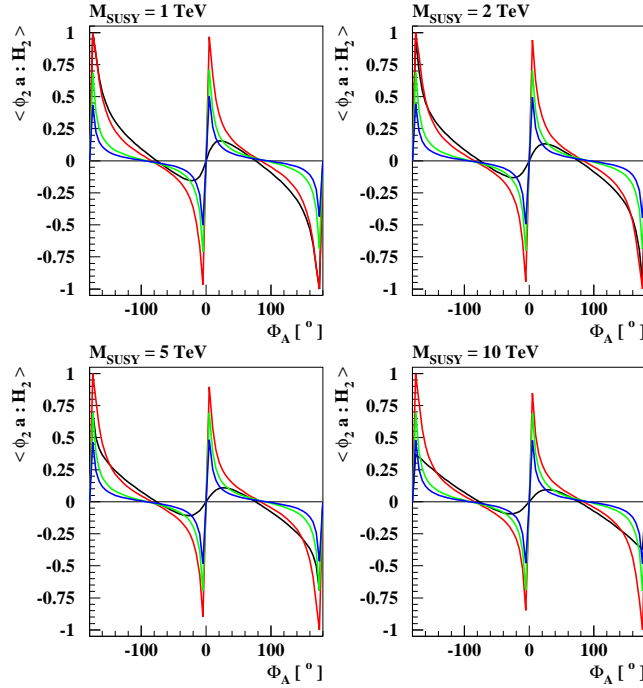


Figure 12: As in Figure 9, but showing the CP mixing quantity  $\frac{2O_{\phi_22}O_{a2}}{O_{\phi_22}^2+O_{a1}^2}$  for the second mass eigenstate  $H_2$ .

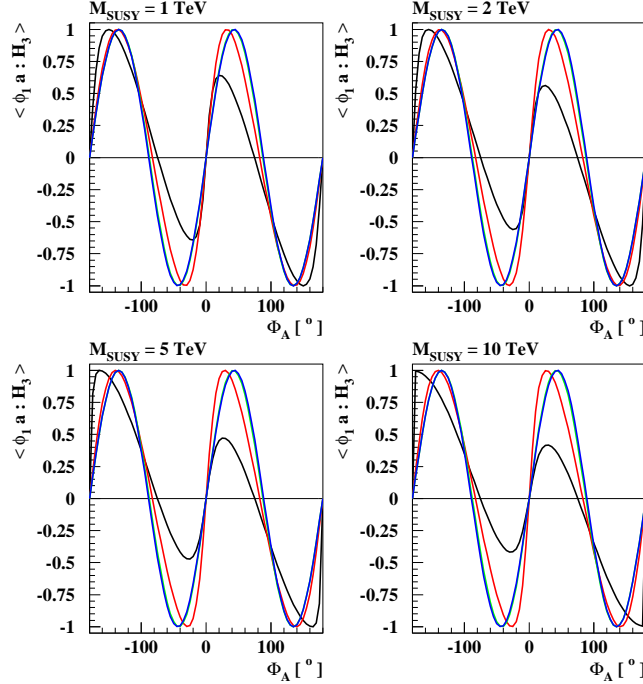


Figure 13: As in Figure 9, but showing the CP mixing quantity  $\frac{2O_{\phi_13}O_{a3}}{O_{\phi_13}^2+O_{a3}^2}$  for the third mass eigenstate  $H_3$ .

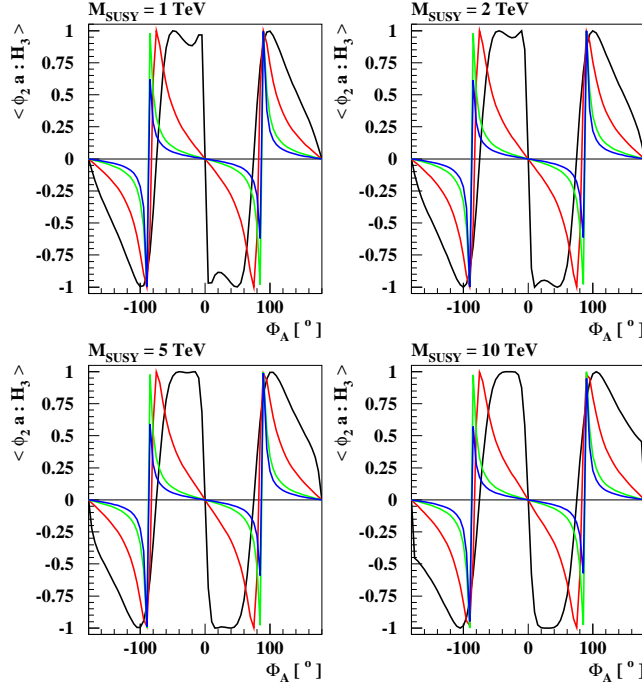


Figure 14: As in Figure 9, but showing the CP mixing quantity  $\frac{2O_{\phi_23}O_{a3}}{O_{\phi_23}^2+O_{a3}^2}$  for the third mass eigenstate  $H_3$ .

## Appendices

In the appendices that follow, we present the relevant Renormalization Group Equations (RGEs) that are applicable above the three typical thresholds: (i) the top-quark mass  $m_t$ , (ii) the heavy Higgs mass  $M_H \equiv M_{H^+}$ , and (iii) the soft SUSY-breaking scale  $M_S$ .

It is convenient to write the RGEs in the form

$$\frac{dc}{dt} = \sum_{n=1} \kappa^n \beta_c^{(n)},$$

where  $c$  stands for any kinematic parameter, such as quartic, gauge and Yukawa couplings, anomalous dimensions, and  $\tan\beta$ . In addition, we use the abbreviations:  $t \equiv \ln Q$  and  $\kappa = 1/(4\pi)^2$ .

## A SM RGEs

For scales of  $Q$ , for which  $M_{H_1} \sim m_t < Q < M_H$ , one needs to consider the RGEs of the SM. To properly take into consideration intermediate particle threshold effects, we introduce the short-hand notation for the step function

$$\Theta_X \equiv \begin{cases} 1 & \text{for } Q \geq M_X, \\ 0 & \text{for } Q < M_X. \end{cases}$$

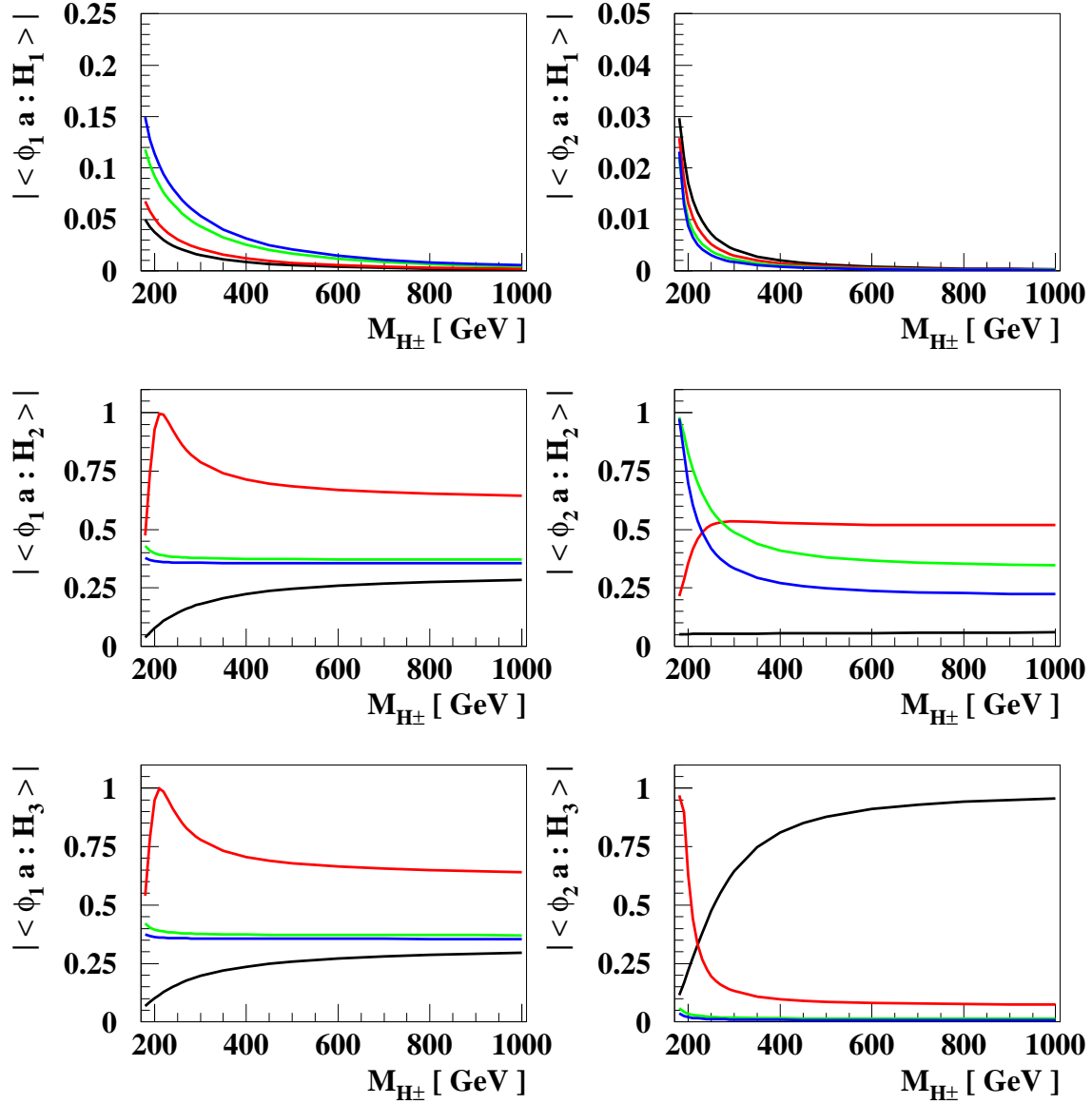


Figure 15: The magnitudes of the mixing quantities  $|\langle \phi_1 a : H_i \rangle|$  (left) and  $|\langle \phi_2 a : H_i \rangle|$  (right), defined in (36), as functions of  $M_{H^\pm}$  for  $M_S = 10$  TeV and  $\Phi_A = 10^\circ$ . The black, red, green and blue lines are for  $\tan\beta = 5, 10, 30$  and  $50$ , respectively.

Upon neglecting the Yukawa couplings of the first two generations of quarks and leptons, the one-loop SM RGEs that we use [35, 42] read:

$$\begin{aligned}
\beta_\lambda^{(1)} = & 12\lambda^2 + 4\lambda(3y_t^2 + 3y_b^2 + y_\tau^2) - 4(3y_t^4 + 3y_b^4 + y_\tau^4) \\
& - 9\lambda \left( g^2 + \frac{1}{3}g'^2 \right) + \frac{9}{4} \left( g^4 + \frac{2}{3}g'^2g^2 + \frac{1}{3}g'^4 \right) \\
& + \left( 6\lambda g^2 - 5g^4 + 8g^4s_\beta^2c_\beta^2 \right) \Theta_{\tilde{H}}\Theta_{\tilde{W}} \\
& - 2g^2g'^2\Theta_{\tilde{H}}\Theta_{\tilde{W}}\Theta_{\tilde{B}} + \left( 2\lambda g'^2 - g'^4 \right) \Theta_{\tilde{H}}\Theta_{\tilde{B}}, \tag{A.1}
\end{aligned}$$

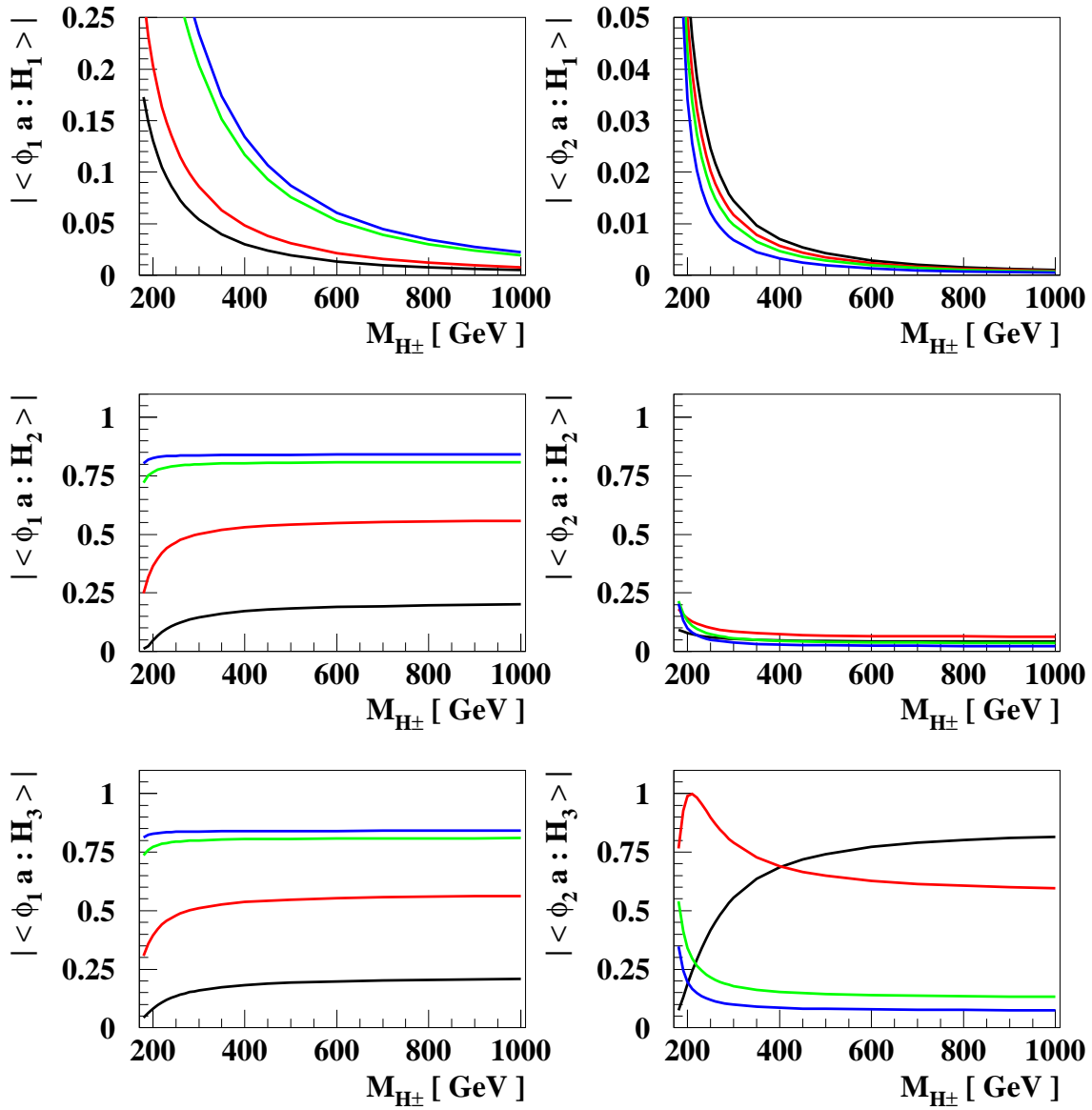


Figure 16: As in Figure 15 but for  $M_S = 10$  TeV and  $\Phi_A = 60^\circ$ .

$$\beta_\lambda^{(2)} = -78\lambda^3 - 72\lambda^2 y_t^2 + 80\lambda g_s^2 y_t^2 - 3\lambda y_t^4 - 64g_s^2 y_t^4 + 60y_t^6, \quad (\text{A.2})$$

$$\begin{aligned} \beta_\lambda^{(3)} = & \frac{\lambda^3}{2} \left( 6011.35 \frac{\lambda}{2} + 873y_t^2 \right) + \lambda^2 y_t^2 (1768.26 y_t^2 + 160.77 g_s^2) \\ & + 2\lambda y_t^2 (-223.382 y_t^4 - 662.866 g_s^2 y_t^2 + 356.968 g_s^4) \\ & + 4y_t^4 (-243.149 y_t^4 + 250.494 g_s^2 y_t^2 - 50.201 g_s^4), \end{aligned} \quad (\text{A.3})$$

$$\beta_{g_s}^{(1)} = -g_s^3 \left[ 11 - \frac{2}{3} N_f \right], \quad (\text{A.4})$$

$$\beta_{g_s}^{(2)} = -g_s^3 \left[ \left( 102 - \frac{38}{3} N_f \right) g_s^2 - \frac{3}{4} N_f g^2 - \frac{11}{36} N_f g'^2 + 2y_t^2 + 2y_b^2 \right], \quad (\text{A.5})$$

$$\begin{aligned} \beta_{y_t}^{(1)} = & y_t \left[ \frac{9}{2} y_t^2 + \frac{3}{2} y_b^2 + y_\tau^2 - 8g_s^2 - \frac{9}{4} g^2 - \frac{17}{12} g'^2 \right] \\ & + \frac{3}{2} y_t g^2 \Theta_{\tilde{H}} \Theta_{\tilde{W}} + \frac{1}{2} y_t g'^2 \Theta_{\tilde{H}} \Theta_{\tilde{B}}, \end{aligned} \quad (\text{A.6})$$

$$\beta_{y_t}^{(2)} = y_t \left[ \frac{3}{2} \lambda^2 - 6\lambda y_t^2 - \left( \frac{404}{3} - \frac{40}{9} N_f \right) g_s^4 + 36g_s^2 y_t^2 - 12y_t^4 \right], \quad (\text{A.7})$$

$$\begin{aligned} \beta_{y_t}^{(3)} = & y_t \left[ -\frac{9}{2} \lambda^3 + \frac{15}{16} \lambda^2 y_t^2 + \lambda y_t^2 (99y_t^2 + 8g_s^2) \right. \\ & \left. + 58.6028 y_t^6 - 157 y_t^4 g_s^2 + 363.764 y_t^2 g_s^4 - 619.35 g_s^6 \right], \end{aligned} \quad (\text{A.8})$$

$$\beta_{y_b}^{(1)} = y_b \left[ \frac{3}{2} y_t^2 + \frac{9}{2} y_b^2 + y_\tau^2 - 8g_s^2 - \frac{9}{4} g^2 - \frac{5}{12} g'^2 \right], \quad (\text{A.9})$$

$$\beta_{y_\tau}^{(1)} = y_\tau \left[ 3y_t^2 + 3y_b^2 + \frac{5}{2} y_\tau^2 - \frac{9}{4} g^2 - \frac{45}{12} g'^2 \right], \quad (\text{A.10})$$

$$\begin{aligned} \beta_{g'}^{(1)} = & \left( \frac{2}{3} N_f + \frac{1}{10} \right) \frac{5}{3} g'^3, \\ \beta_{g'}^{(2)} = & \left( \frac{22}{9} N_f g_s^2 - \frac{17}{6} y_t^2 \right) g'^3, \\ \beta_g^{(1)} = & \left( -\frac{22}{3} + \frac{2}{3} N_f + \frac{1}{6} \right) g^3, \\ \beta_g^{(2)} = & \left( 2N_f g_s^2 - \frac{3}{2} y_t^2 \right) g^3, \end{aligned} \quad (\text{A.11})$$

$$\gamma^{(1)} = \frac{9}{4} \left( g^2 + \frac{1}{3} g'^2 \right) - (3y_t^2 + 3y_b^2 + y_\tau^2). \quad (\text{A.12})$$

## B One-Loop 2HDM RGEs

For RG scales  $Q$  between  $M_H$  and  $M_S$ , the effective theory becomes a general 2HDM, whilst for  $Q > M_S$  the theory becomes fully supersymmetric and the quartic couplings  $\lambda_{5,6,7}$  do not run. Here, we give the RGEs of the general 2HDM at the one-loop level, and relegate to Appendix C the presentation of the two-loop results.

As before, we neglect the Yukawa couplings of the first two generations of quarks and leptons, and note that in addition to the change of normalizations given in (5), we use

$t = \ln(Q)$  instead of  $\ln(Q^2)$  as used in Ref. [31]. Thus, adapting the results of [31], the one-loop 2HDM RGEs may be listed as follows:

$$\begin{aligned}
\beta_{\lambda_1}^{(1)} = & - \left\{ 24\lambda_1^2 + \lambda_3^2 + (\lambda_3 + \lambda_4)^2 + 4\lambda_5^2 + 12\lambda_6^2 + \frac{3}{8}[2g^4 + (g^2 + g'^2)^2] \right\} \Theta_Z \\
& - N_C \left\{ -2h_b^4 \Theta_Z + \left( h_b^2 - \frac{1}{4}g'^2 Y_D \right)^2 \Theta_{\tilde{D}_3} + \left( \frac{1}{4}g'^2 Y_U \right)^2 \Theta_{\tilde{U}_3} \right. \\
& \quad \left. + \left[ h_b^4 - \frac{1}{2}h_b^2(g'^2 Y_Q + g^2) + \frac{1}{8}(g^4 + g'^4 Y_Q^2) \right] \Theta_{\tilde{Q}_3} \right\} \\
& - N_C \sum_{i=1}^2 \left\{ \left( \frac{1}{4}g'^2 Y_D \right)^2 \Theta_{\tilde{D}_i} + \left( \frac{1}{4}g'^2 Y_U \right)^2 \Theta_{\tilde{U}_i} + \frac{1}{8}(g^4 + g'^4 Y_Q^2) \Theta_{\tilde{Q}_i} \right\} \\
& - \left\{ -2h_\tau^4 \Theta_Z + \left( h_\tau^2 - \frac{1}{4}g'^2 Y_E \right)^2 \Theta_{\tilde{E}_3} + \left[ h_\tau^4 - \frac{1}{2}h_\tau^2(g'^2 Y_L + g^2) + \frac{1}{8}(g^4 + g'^4 Y_L^2) \right] \Theta_{\tilde{L}_3} \right\} \\
& - \sum_{i=1}^2 \left\{ \left( \frac{1}{4}g'^2 Y_E \right)^2 \Theta_{\tilde{E}_i} + \frac{1}{8}(g^4 + g'^4 Y_L^2) \Theta_{\tilde{L}_i} \right\} \\
& + \frac{5}{2}g^4 \Theta_{\tilde{H}} \Theta_{\tilde{W}} + g'^2 g^2 \Theta_{\tilde{H}} \Theta_{\tilde{W}} \Theta_{\tilde{B}} + \frac{1}{2}g'^4 \Theta_{\tilde{H}} \Theta_{\tilde{B}} - 4\lambda_1 \gamma_1^{(1)}, \tag{B.1}
\end{aligned}$$

where  $N_C = 3$ ,  $Y_Q = 1/3$ ,  $Y_U = -4/3$ ,  $Y_D = 2/3$ ,  $Y_L = -1$ ,  $Y_E = 2$ , and

$$\begin{aligned}
\beta_{\lambda_2}^{(1)} = & - \left\{ 24\lambda_2^2 + \lambda_3^2 + (\lambda_3 + \lambda_4)^2 + 4\lambda_5^2 + 12\lambda_6^2 + \frac{3}{8}[2g^4 + (g^2 + g'^2)^2] \right\} \Theta_Z \\
& - N_C \left\{ -2h_t^4 \Theta_t \Theta_Z + \left( \frac{1}{4}g'^2 Y_D \right)^2 \Theta_{\tilde{D}_3} + \left( h_t^2 + \frac{1}{4}g'^2 Y_U \right)^2 \Theta_{\tilde{U}_3} \right. \\
& \quad \left. + \left[ h_t^4 + \frac{1}{2}h_t^2(g'^2 Y_Q - g^2) + \frac{1}{8}(g^4 + g'^4 Y_Q^2) \right] \Theta_{\tilde{Q}_3} \right\} \\
& - N_C \sum_{i=1}^2 \left\{ \left( \frac{1}{4}g'^2 Y_D \right)^2 \Theta_{\tilde{D}_i} + \left( \frac{1}{4}g'^2 Y_U \right)^2 \Theta_{\tilde{U}_i} + \frac{1}{8}(g^4 + g'^4 Y_Q^2) \Theta_{\tilde{Q}_i} \right\} \\
& - \sum_{i=1}^3 \left\{ \left( \frac{1}{4}g'^2 Y_E \right)^2 \Theta_{\tilde{E}_i} + \frac{1}{8}(g^4 + g'^4 Y_L^2) \Theta_{\tilde{L}_i} \right\} \\
& + \frac{5}{2}g^4 \Theta_{\tilde{H}} \Theta_{\tilde{W}} + g'^2 g^2 \Theta_{\tilde{H}} \Theta_{\tilde{W}} \Theta_{\tilde{B}} + \frac{1}{2}g'^4 \Theta_{\tilde{H}} \Theta_{\tilde{B}} - 4\lambda_2 \gamma_2^{(1)}, \tag{B.2}
\end{aligned}$$

$$\begin{aligned}
\beta_{\lambda_3}^{(1)} = & -2 \left\{ 2(\lambda_1 + \lambda_2)(3\lambda_3 + \lambda_4) + 2\lambda_3^2 + \lambda_4^2 + 4\lambda_5^2 + 2\lambda_6^2 + 2\lambda_7^2 + 8\lambda_6 \lambda_7 \right. \\
& \quad \left. + \frac{3}{8}[2g^4 + (g^2 - g'^2)^2] \right\} \Theta_Z \\
& - 2N_C \left\{ -2h_t^2 h_b^2 \Theta_t \Theta_Z + \frac{1}{4}g'^2 Y_D \left( h_b^2 - \frac{1}{4}g'^2 Y_D \right) \Theta_{\tilde{D}_3} \right. \\
& \quad \left. - \frac{1}{4}g'^2 Y_U \left( h_t^2 + \frac{1}{4}g'^2 Y_U \right) \Theta_{\tilde{U}_3} + h_t^2 h_b^2 \Theta_{\tilde{U}_3} \Theta_{\tilde{D}_3} \right\}
\end{aligned}$$

$$\begin{aligned}
& + \left[ h_t^2 h_b^2 - \frac{1}{4} h_t^2 (g'^2 Y_Q + g^2) + \frac{1}{4} h_b^2 (g'^2 Y_Q - g^2) + \frac{1}{8} (g^4 - g'^4 Y_Q^2) \right] \Theta_{\tilde{Q}_3} \Big\} \\
& - 2N_C \sum_{i=1}^2 \left\{ - \left( \frac{1}{4} g'^2 Y_D \right)^2 \Theta_{\tilde{D}_i} - \left( \frac{1}{4} g'^2 Y_U \right)^2 \Theta_{\tilde{U}_i} + \frac{1}{8} (g^4 - g'^4 Y_Q^2) \Theta_{\tilde{Q}_i} \right\} \\
& - 2 \left\{ \frac{1}{4} g'^2 Y_E \left( h_\tau^2 - \frac{1}{4} g'^2 Y_E \right) \Theta_{\tilde{E}_3} + \left[ \frac{1}{4} h_\tau^2 (g'^2 Y_L - g^2) + \frac{1}{8} (g^4 - g'^4 Y_L^2) \right] \Theta_{\tilde{L}_3} \right\} \\
& - 2 \sum_{i=1}^2 \left\{ - \left( \frac{1}{4} g'^2 Y_E \right)^2 \Theta_{\tilde{E}_i} + \frac{1}{8} (g^4 - g'^4 Y_L^2) \Theta_{\tilde{L}_i} \right\} \\
& + 5g^4 \Theta_{\tilde{W}} \Theta_{\tilde{H}} - 2g'^2 g^2 \Theta_{\tilde{W}} \Theta_{\tilde{B}} \Theta_{\tilde{H}} + g'^4 \Theta_{\tilde{B}} \Theta_{\tilde{H}} - 2\lambda_3 (\gamma_1^{(1)} + \gamma_2^{(1)}) , \tag{B.3}
\end{aligned}$$

$$\begin{aligned}
\beta_{\lambda_4}^{(1)} = & -2 \left[ \lambda_4 (2\lambda_1 + 2\lambda_2 + 4\lambda_3 + 2\lambda_4) + 16\lambda_5^2 + 5\lambda_6^2 + 5\lambda_7^2 + 2\lambda_6\lambda_7 + \frac{3}{2}g^2 g'^2 \right] \Theta_Z \\
& - 2N_C \left\{ 2h_t^2 h_b^2 \Theta_t \Theta_Z - h_t^2 h_b^2 \Theta_{\tilde{U}_3} \Theta_{\tilde{D}_3} - \left( h_t^2 - \frac{1}{2}g^2 \right) \left( h_b^2 - \frac{1}{2}g^2 \right) \Theta_{\tilde{Q}_3} \right\} \\
& + 2N_C \sum_{i=1}^2 \left( \frac{1}{2}g^2 \right)^2 \Theta_{\tilde{Q}_i} - g^2 \left( h_\tau^2 - \frac{1}{2}g^2 \right) \Theta_{\tilde{L}_3} + \sum_{i=1}^2 \frac{1}{2}g^4 \Theta_{\tilde{L}_i} \\
& - 4g^4 \Theta_{\tilde{W}} \Theta_{\tilde{H}} + 4g'^2 g^2 \Theta_{\tilde{W}} \Theta_{\tilde{B}} \Theta_{\tilde{H}} - 2\lambda_4 (\gamma_1^{(1)} + \gamma_2^{(1)}) , \tag{B.4}
\end{aligned}$$

$$\begin{aligned}
\beta_{\lambda_5}^{(1)} = & - \left[ 2\lambda_5 (2\lambda_1 + 2\lambda_2 + 4\lambda_3 + 6\lambda_4) + 5 (\lambda_6^2 + \lambda_7^2) + 2\lambda_6\lambda_7 \right] \Theta_Z - 2\lambda_5 (\gamma_1^{(1)} + \gamma_2^{(1)}) , \tag{B.5}
\end{aligned}$$

$$\begin{aligned}
\beta_{\lambda_6}^{(1)} = & -2 [\lambda_6 (12\lambda_1 + 3\lambda_3 + 4\lambda_4 + 10\lambda_5) + \lambda_7 (3\lambda_3 + 2\lambda_4 + 2\lambda_5)] \Theta_Z - \lambda_6 (3\gamma_1^{(1)} + \gamma_2^{(1)}) , \tag{B.6}
\end{aligned}$$

$$\begin{aligned}
\beta_{\lambda_7}^{(1)} = & -2 [\lambda_7 (12\lambda_2 + 3\lambda_3 + 4\lambda_4 + 10\lambda_5) + \lambda_6 (3\lambda_3 + 2\lambda_4 + 2\lambda_5)] \Theta_Z - \lambda_7 (\gamma_1^{(1)} + 3\gamma_2^{(1)}) , \tag{B.7}
\end{aligned}$$

$$\gamma_1^{(1)} = \frac{1}{4} \left[ (9g^2 + 3g'^2 - 4(N_C h_b^2 + h_\tau^2)) \Theta_Z - 6g^2 \Theta_{\tilde{W}} \Theta_{\tilde{H}} - 2g'^2 \Theta_{\tilde{B}} \Theta_{\tilde{H}} \right] , \tag{B.8}$$

$$\gamma_2^{(1)} = \frac{1}{4} \left[ (9g^2 + 3g'^2 - 4N_C h_t^2 \Theta_t) \Theta_Z - 6g^2 \Theta_{\tilde{W}} \Theta_{\tilde{H}} - 2g'^2 \Theta_{\tilde{B}} \Theta_{\tilde{H}} \right] , \tag{B.9}$$

$$\beta_{h_t}^{(1)} = \left( \frac{9}{2} h_t^2 + \frac{1}{2} h_b^2 - 8g_s^2 - \frac{9}{4}g^2 - \frac{17}{12}g'^2 \right) h_t , \tag{B.10}$$

$$\beta_{h_b}^{(1)} = \left( \frac{9}{2} h_b^2 + \frac{1}{2} h_t^2 + h_\tau^2 - 8g_s^2 - \frac{9}{4}g^2 - \frac{5}{12}g'^2 \right) h_b , \tag{B.11}$$

$$\beta_{h_\tau}^{(1)} = \left( \frac{5}{2} h_\tau^2 + 3h_b^2 - \frac{9}{4}g^2 - \frac{15}{4}g'^2 \right) h_\tau , \tag{B.12}$$

$$\begin{aligned}
\beta_{g'}^{(1)} = & \left\{ \frac{1}{4} N_C \sum_{i=1}^3 \left[ 2Y_Q^2 (2\Theta_t + \Theta_{\tilde{Q}_i}) + Y_U^2 (2\Theta_t + \Theta_{\tilde{U}_i}) + Y_D^2 (2\Theta_t + \Theta_{\tilde{D}_i}) \right] \right. \\
& \left. + \frac{1}{4} \sum_{i=1}^3 \left[ 2Y_L^2 (2\Theta_t + \Theta_{\tilde{L}_i}) + Y_E^2 (2\Theta_t + \Theta_{\tilde{E}_i}) \right] + \frac{1}{2} N_H \Theta_t + N_{\tilde{H}} \Theta_{\tilde{H}} \right\} \frac{g'^3}{3} ,
\end{aligned} \tag{B.13}$$

with  $N_H = 2$  and  $N_{\tilde{H}} = 2$ ,

$$\beta_g^{(1)} = \left\{ \frac{1}{2} N_C \sum_{i=1}^3 (2\Theta_t + \Theta_{\tilde{Q}_i}) + \frac{1}{2} \sum_{i=1}^3 (2\Theta_t + \Theta_{\tilde{L}_i}) + \frac{1}{2} N_H \Theta_t + N_{\tilde{H}} \Theta_{\tilde{H}} + 4N_{\tilde{W}} \Theta_{\tilde{W}} - 22\Theta_t \right\} \frac{g^3}{3} , \tag{B.14}$$

with  $N_{\tilde{W}} = 1$ ,

$$\beta_{g_s}^{(1)} = \left\{ 2N_f + \sum_{i=1}^3 \left( \Theta_{\tilde{Q}_i} + \frac{1}{2} \Theta_{\tilde{U}_i} + \frac{1}{2} \Theta_{\tilde{D}_i} \right) + 6N_{\tilde{g}} \Theta_{\tilde{g}} - 33 \right\} \frac{g_s^3}{3} , \tag{B.15}$$

with  $N_f = \Theta_t + \Theta_b + \Theta_c + \Theta_s + \Theta_d + \Theta_u$  and  $N_{\tilde{g}} = 1$ ,

$$\begin{aligned}
\beta_{\tan \beta}^{(1)} = & (\gamma_2^{(1)} - \gamma_1^{(1)}) \tan \beta \\
= & (-N_C h_t^2 \Theta_t \Theta_Z + N_C h_b^2 \Theta_Z + h_\tau^2 \Theta_Z) \tan \beta ,
\end{aligned} \tag{B.16}$$

$$\beta_{\mu_1^2}^{(1)} = -2 \left[ 6\mu_1^2 \lambda_1 + \mu_2^2 (2\lambda_3 + \lambda_4) + 6m_{12}^2 \lambda_6 \right] - 2\gamma_1^{(1)} \mu_1^2 , \tag{B.17}$$

$$\beta_{\mu_2^2}^{(1)} = -2 \left[ 6\mu_2^2 \lambda_2 + \mu_1^2 (2\lambda_3 + \lambda_4) + 6m_{12}^2 \lambda_7 \right] - 2\gamma_2^{(1)} \mu_2^2 , \tag{B.18}$$

$$\beta_{m_{12}^2}^{(1)} = 2 \left[ -(\lambda_3 + 2\lambda_4 + 6\lambda_5) m_{12}^2 - 3\lambda_6 \mu_1^2 - 3\lambda_7 \mu_2^2 \right] - (\gamma_1^{(1)} + \gamma_2^{(1)}) m_{12}^2 . \tag{B.19}$$

## C Two-Loop 2HDM RGEs

In this appendix, we present the RGEs of the general 2HDM at the two-loop order, as derived in [32, 33]. For definiteness, we follow the conventions of [33], where  $g_3 \rightarrow g_s$ ,  $g_2 \rightarrow g$ ,  $g_1^2 \rightarrow (5/3)g'^2$ ;  $\lambda_{1,2,5} \rightarrow -2\lambda_{1,2,5}$ ,  $\lambda_{3,4,6,7} \rightarrow -\lambda_{3,4,6,7}$ . The two-loop beta functions for the quartic couplings are given by

$$\begin{aligned}
\beta_{\lambda_1}^{(2)} = & -\frac{291}{16} g^6 + \frac{101}{16} g^4 g'^2 + \frac{191}{16} g^2 g'^4 + \frac{131}{16} g'^6 \\
& + \frac{3}{16} g^4 \left[ 12h_b^2 + 4h_\tau^2 - 34\lambda_1 + 20(2\lambda_3 + \lambda_4) \right] - \frac{1}{8} g^2 g'^2 \left[ 36h_b^2 + 44h_\tau^2 - 78\lambda_1 - 20\lambda_4 \right]
\end{aligned}$$

$$\begin{aligned}
& -\frac{1}{16}g'^4 \left[ 20h_b^2 - 100h_\tau^2 - 434\lambda_1 - 20(2\lambda_3 + \lambda_4) \right] \\
& + 8g_s^2 h_b^2 \left[ 4h_b^2 + 10\lambda_1 \right] - \frac{3}{4}g^2 \left[ -10\lambda_1(3h_b^2 + h_\tau^2) + 4(36\lambda_1^2 + 4\lambda_3^2 + 4\lambda_3\lambda_4 + \lambda_4^2 + 18\lambda_6^2) \right] \\
& - \frac{1}{12}g'^2 \left[ h_b^2(16h_b^2 - 50\lambda_1) + 3h_\tau^2(-16h_\tau^2 - 50\lambda_1) \right. \\
& \quad \left. + 12(36\lambda_1^2 + 4\lambda_3^2 + 4\lambda_3\lambda_4 + 2\lambda_4^2 - 4\lambda_5^2 + 18\lambda_6^2) \right] \\
& + 6h_t^2 \left[ 2\lambda_3^2 + 2\lambda_3\lambda_4 + \lambda_4^2 + 4\lambda_5^2 + 6\lambda_6^2 \right] - \frac{3}{2}h_t^2 h_b^2 \left[ 4h_b^2 + 6\lambda_1 \right] \\
& + \frac{3}{2}h_b^2 \left[ -20h_b^4 - 2h_b^2\lambda_1 + 96\lambda_1^2 + 24\lambda_6^2 \right] + \frac{1}{2}h_\tau^2 \left[ -20h_\tau^4 - 2h_\tau^2\lambda_1 + 96\lambda_1^2 + 24\lambda_6^2 \right] \\
& - 2\lambda_1 \left[ 156\lambda_1^2 + 10\lambda_3^2 + 10\lambda_3\lambda_4 + 6\lambda_4^2 + 28\lambda_5^2 + 159\lambda_6^2 - 3\lambda_7^2 \right] \\
& - 2\lambda_3 \left[ 4\lambda_3^2 + 6\lambda_3\lambda_4 + 8\lambda_4^2 + 40\lambda_5^2 + 33\lambda_6^2 + 18\lambda_6\lambda_7 + 9\lambda_7^2 \right] \\
& - 2\lambda_4 \left[ 3\lambda_4^2 + 44\lambda_5^2 + 35\lambda_6^2 + 14\lambda_6\lambda_7 + 7\lambda_7^2 \right] - 4\lambda_5 \left[ 37\lambda_6^2 + 10\lambda_6\lambda_7 + 5\lambda_7^2 \right], \quad (C.1)
\end{aligned}$$

$$\begin{aligned}
\beta_{\lambda_2}^{(2)} = & -\frac{291}{16}g^6 + \frac{101}{16}g^4g'^2 + \frac{191}{16}g^2g'^4 + \frac{131}{16}g'^6 \\
& + \frac{3}{16}g^4 \left[ 12h_t^2 - 34\lambda_2 + 20(2\lambda_3 + \lambda_4) \right] - \frac{1}{8}g^2g'^2 \left[ 84h_t^2 - 78\lambda_2 - 20\lambda_4 \right] \\
& + \frac{1}{16}g'^4 \left[ 76h_t^2 + 434\lambda_2 + 20(2\lambda_3 + \lambda_4) \right] \\
& + 8g_s^2 h_t^2 \left[ 4h_t^2 + 10\lambda_2 \right] - \frac{3}{4}g^2 \left[ -30h_t^2\lambda_2 + 4(36\lambda_2^2 + 4\lambda_3^2 + 4\lambda_3\lambda_4 + \lambda_4^2 + 18\lambda_7^2) \right] \\
& - \frac{1}{12}g'^2 \left[ -h_t^2(32h_t^2 + 170\lambda_2) + 12(36\lambda_2^2 + 4\lambda_3^2 + 4\lambda_3\lambda_4 + 2\lambda_4^2 - 4\lambda_5^2 + 18\lambda_7^2) \right] \\
& - \frac{3}{2}h_t^2 \left[ 20h_t^4 + 2h_t^2\lambda_2 - 96\lambda_2^2 - 24\lambda_7^2 \right] - \frac{3}{2}h_t^2 h_b^2 \left[ 4h_b^2 + 6\lambda_2 \right] \\
& + (6h_b^2 + 2h_\tau^2) \left[ 2\lambda_3^2 + 2\lambda_3\lambda_4 + \lambda_4^2 + 4\lambda_5^2 + 6\lambda_7^2 \right] \\
& - 2\lambda_2 \left[ 156\lambda_2^2 + 10\lambda_3^2 + 10\lambda_3\lambda_4 + 6\lambda_4^2 + 28\lambda_5^2 - 3\lambda_6^2 + 159\lambda_7^2 \right] \\
& - 2\lambda_3 \left[ 4\lambda_3^2 + 6\lambda_3\lambda_4 + 8\lambda_4^2 + 40\lambda_5^2 + 9\lambda_6^2 + 18\lambda_6\lambda_7 + 33\lambda_7^2 \right] \\
& - 2\lambda_4 \left[ 3\lambda_4^2 + 44\lambda_5^2 + 7\lambda_6^2 + 14\lambda_6\lambda_7 + 35\lambda_7^2 \right] - 4\lambda_5 \left[ 5\lambda_6^2 + 10\lambda_6\lambda_7 + 37\lambda_7^2 \right], \quad (C.2)
\end{aligned}$$

$$\begin{aligned}
\beta_{\lambda_3}^{(2)} = & -\frac{291}{8}g^6 - \frac{11}{8}g^4g'^2 - \frac{101}{8}g^2g'^4 + \frac{131}{8}g'^6 \\
& + \frac{3}{4}g^4 \left[ 3h_t^2 + 3h_b^2 + h_\tau^2 + 30(\lambda_1 + \lambda_2) - \frac{37}{2}\lambda_3 + 10\lambda_4 \right] \\
& + \frac{1}{2}g^2g'^2 \left[ 21h_t^2 + 9h_b^2 + 11h_\tau^2 - 10(\lambda_1 + \lambda_2) + \frac{11}{2}\lambda_3 - 6\lambda_4 \right] \\
& - \frac{1}{8}g'^4 \left[ -38h_t^2 + 10h_b^2 - 50h_\tau^2 - 60(\lambda_1 + \lambda_2) - 197\lambda_3 - 20\lambda_4 \right] \\
& + 8g_s^2 \left[ 8h_t^2 h_b^2 + 5\lambda_3(h_t^2 + h_b^2) \right]
\end{aligned}$$

$$\begin{aligned}
& -6g^2 \left[ -\frac{5}{8}\lambda_3(3h_t^2 + 3h_b^2 + h_\tau^2) + 6(\lambda_1 + \lambda_2)(2\lambda_3 + \lambda_4) + (\lambda_3 - \lambda_4)^2 + 18\lambda_6\lambda_7 \right] \\
& -\frac{1}{3}g'^2 \left[ -4h_t^2h_b^2 - \frac{5}{4}\lambda_3(17h_t^2 + 5h_b^2 + 15h_\tau^2) \right. \\
& \quad \left. + 24(\lambda_1 + \lambda_2)(3\lambda_3 + \lambda_4) + 6(\lambda_3^2 - \lambda_4^2 + 8\lambda_5^2 + \lambda_6^2 + 16\lambda_6\lambda_7 + \lambda_7^2) \right] \\
& + \frac{9}{2}\lambda_3 \left[ 3h_t^4 + 3h_b^4 + h_\tau^4 \right] - h_t^2h_b^2 \left[ 36(h_t^2 + h_b^2) - 15\lambda_3 \right] \\
& + 6h_t^2 \left[ 12\lambda_2\lambda_3 + 4\lambda_2\lambda_4 + 2\lambda_3^2 + \lambda_4^2 + 4\lambda_5^2 + 8\lambda_6\lambda_7 + 4\lambda_7^2 \right] \\
& + (6h_b^2 + 2h_\tau^2) \left[ 12\lambda_1\lambda_3 + 4\lambda_1\lambda_4 + 2\lambda_3^2 + \lambda_4^2 + 4\lambda_5^2 + 4\lambda_6^2 + 8\lambda_6\lambda_7 \right] \\
& - 4(\lambda_1^2 + \lambda_2^2) [15\lambda_3 + 4\lambda_4] - 4(\lambda_1 + \lambda_2) [18\lambda_3^2 + 8\lambda_3\lambda_4 + 7\lambda_4^2 + 36\lambda_5^2] \\
& - 4\lambda_1 [31\lambda_6^2 + 22\lambda_6\lambda_7 + 11\lambda_7^2] - 4\lambda_2 [11\lambda_6^2 + 22\lambda_6\lambda_7 + 31\lambda_7^2] \\
& - \lambda_3 [12\lambda_3^2 + 4\lambda_3\lambda_4 + 16\lambda_4^2 + 72\lambda_5^2 + 60\lambda_6^2 + 176\lambda_6\lambda_7 + 60\lambda_7^2] \\
& - \lambda_4 [12\lambda_4^2 + 176\lambda_5^2 + 68\lambda_6^2 + 88\lambda_6\lambda_7 + 68\lambda_7^2] \\
& - 2\lambda_5 [68\lambda_6^2 + 72\lambda_6\lambda_7 + 68\lambda_7^2] , \tag{C.3}
\end{aligned}$$

$$\begin{aligned}
\beta_{\lambda_4}^{(2)} = & +14g^4g'^2 + \frac{73}{2}g^2g'^4 + \lambda_4 \left[ -\frac{231}{8}g^4 + \frac{157}{8}g'^4 \right] \\
& -\frac{1}{2}g^2g'^2 \left[ 42h_t^2 + 18h_b^2 + 22h_\tau^2 - 20\lambda_1 - 20\lambda_2 - 4\lambda_3 - \frac{51}{2}\lambda_4 \right] \\
& -8g_s^2 \left[ 8h_t^2h_b^2 - 5\lambda_4(h_t^2 + h_b^2) \right] \\
& -g^2 \left[ -\frac{15}{4}\lambda_4(3h_t^2 + 3h_b^2 + h_\tau^2) + 18(2\lambda_3\lambda_4 + \lambda_4^2 + 12\lambda_5^2 + 3\lambda_6^2 + 3\lambda_7^2) \right] \\
& -\frac{1}{3}g'^2 \left[ 4h_t^2h_b^2 - \frac{5}{4}\lambda_4(17h_t^2 + 5h_b^2 + 15h_\tau^2) + 12\lambda_4(2\lambda_1 + 2\lambda_2 + \lambda_3 + 2\lambda_4) \right. \\
& \quad \left. + 6(32\lambda_5^2 + 7\lambda_6^2 + 4\lambda_6\lambda_7 + 7\lambda_7^2) \right] \\
& -\frac{9}{2}\lambda_4 \left[ 3h_t^4 + 3h_b^4 + h_\tau^4 \right] + h_t^2h_b^2 \left[ 24(h_t^2 + h_b^2) - 24\lambda_3 - 33\lambda_4 \right] \\
& + 12h_t^2 \left[ 2\lambda_2\lambda_4 + 2\lambda_3\lambda_4 + \lambda_4^2 + 8\lambda_5^2 + \lambda_6\lambda_7 + 5\lambda_7^2 \right] \\
& + (12h_b^2 + 4h_\tau^2) \left[ 2\lambda_1\lambda_4 + 2\lambda_3\lambda_4 + \lambda_4^2 + 8\lambda_5^2 + 5\lambda_6^2 + \lambda_6\lambda_7 \right] \\
& - 28\lambda_4 [\lambda_1^2 + \lambda_2^2] - 8(\lambda_1 + \lambda_2) [10\lambda_3\lambda_4 + 5\lambda_4^2 + 24\lambda_5^2] \\
& - 4\lambda_1 [37\lambda_6^2 + 10\lambda_6\lambda_7 + 5\lambda_7^2] - 4\lambda_2 [5\lambda_6^2 + 10\lambda_6\lambda_7 + 37\lambda_7^2] \\
& - 4\lambda_3 [7\lambda_3\lambda_4 + 7\lambda_4^2 + 48\lambda_5^2 + 18\lambda_6^2 + 20\lambda_6\lambda_7 + 18\lambda_7^2] \\
& - 2\lambda_4 [52\lambda_5^2 + 34\lambda_6^2 + 80\lambda_6\lambda_7 + 34\lambda_7^2] - 32\lambda_5 [5\lambda_6^2 + 6\lambda_6\lambda_7 + 5\lambda_7^2] , \tag{C.4}
\end{aligned}$$

$$\beta_{\lambda_5}^{(2)} = +\lambda_5 \left[ -\frac{231}{8}g^4 + \frac{19}{4}g^2g'^2 + \frac{157}{8}g'^4 \right] + 40g_s^2\lambda_5 [h_t^2 + h_b^2]$$

$$\begin{aligned}
& -\frac{3}{8}g^2 \left[ -10\lambda_5(3h_t^2 + 3h_b^2 + h_\tau^2) + 96\lambda_5(\lambda_3 + 2\lambda_4) + 72(\lambda_6^2 + \lambda_7^2) \right] \\
& -\frac{1}{24}g'^2 \left[ -10\lambda_5(17h_t^2 + 5h_b^2 + 15h_\tau^2) - 48\lambda_5(2\lambda_1 + 2\lambda_2 - 8\lambda_3 - 12\lambda_4) \right. \\
& \quad \left. + 48(5\lambda_6^2 - \lambda_6\lambda_7 + 5\lambda_7^2) \right] \\
& -\frac{1}{2}\lambda_5 \left[ 3h_t^4 + 3h_b^4 + h_\tau^4 \right] - h_t^2 \left[ 33h_b^2\lambda_5 - 12\lambda_5(2\lambda_2 + 2\lambda_3 + 3\lambda_4) - 6\lambda_7(\lambda_6 + 5\lambda_7) \right] \\
& +(6h_b^2 + 2h_\tau^2) [2\lambda_5(2\lambda_1 + 2\lambda_3 + 3\lambda_4) + \lambda_6(5\lambda_6 + \lambda_7)] \\
& -28\lambda_5 [\lambda_1^2 + \lambda_2^2] - 8\lambda_5(\lambda_1 + \lambda_2)(10\lambda_3 + 11\lambda_4) \\
& -2\lambda_1 [37\lambda_6^2 + 10\lambda_6\lambda_7 + 5\lambda_7^2] - 2\lambda_2 [5\lambda_6^2 + 10\lambda_6\lambda_7 + 37\lambda_7^2] \\
& -2\lambda_3 [14\lambda_3\lambda_5 + 38\lambda_4\lambda_5 + 18\lambda_6^2 + 20\lambda_6\lambda_7 + 18\lambda_7^2] \\
& -2\lambda_4 [16\lambda_4\lambda_5 + 19\lambda_6^2 + 22\lambda_6\lambda_7 + 19\lambda_7^2] + 24\lambda_5^3 - 8\lambda_5 [9\lambda_6^2 + 21\lambda_6\lambda_7 + 9\lambda_7^2] , \quad (C.5)
\end{aligned}$$

$$\begin{aligned}
\beta_{\lambda_6}^{(2)} = & +\frac{1}{8}g^4 [-141\lambda_6 + 90\lambda_7] + \frac{1}{4}g^2g'^2 [29\lambda_6 + 10\lambda_7] + \frac{1}{8}g'^4 [187\lambda_6 + 30\lambda_7] + 20g_s^2\lambda_6 [h_t^2 + 3h_b^2] \\
& +\frac{9}{8}g^2 [5\lambda_6(h_t^2 + 3h_b^2 + h_\tau^2) - 96\lambda_6(\lambda_1 + \lambda_5) - 16\lambda_6(\lambda_3 + 2\lambda_4) - 16\lambda_7(2\lambda_3 + \lambda_4)] \\
& +\frac{1}{24}g'^2 [5\lambda_6(17h_t^2 + 15h_b^2 + 45h_\tau^2) - 48\lambda_6(18\lambda_1 + 3\lambda_3 + 5\lambda_4 + 20\lambda_5) \\
& \quad - 48\lambda_7(6\lambda_3 + 4\lambda_4 - 2\lambda_5)] \\
& -\frac{1}{4}\lambda_6 [27h_t^4 + 84h_t^2h_b^2 + 33h_b^4 + 11h_\tau^4] \\
& +6h_t^2 [\lambda_6(3\lambda_3 + 4\lambda_4 + 10\lambda_5) + \lambda_7(6\lambda_3 + 4\lambda_4 + 4\lambda_5)] \\
& +(6h_b^2 + 2h_\tau^2)\lambda_6 [24\lambda_1 + 3\lambda_3 + 4\lambda_4 + 10\lambda_5] \\
& -6\lambda_6 [53\lambda_1^2 - \lambda_2^2] - 4\lambda_1\lambda_6 [33\lambda_3 + 35\lambda_4 + 74\lambda_5] - 4\lambda_2\lambda_6 [9\lambda_3 + 7\lambda_4 + 10\lambda_5] \\
& -2\lambda_6 [16\lambda_3^2 + 34\lambda_3\lambda_4 + 72\lambda_3\lambda_5 + 17\lambda_4^2 + 76\lambda_4\lambda_5 + 72\lambda_5^2] \\
& -4(\lambda_1 + \lambda_2)\lambda_7 [9\lambda_3 + 7\lambda_4 + 10\lambda_5] \\
& -2\lambda_7 [18\lambda_3^2 + 28\lambda_3\lambda_4 + 40\lambda_3\lambda_5 + 17\lambda_4^2 + 44\lambda_4\lambda_5 + 84\lambda_5^2] \\
& -3 [37\lambda_6^3 + 42\lambda_6^2\lambda_7 + 11\lambda_6\lambda_7^2 + 14\lambda_7^3] , \quad (C.6)
\end{aligned}$$

$$\begin{aligned}
\beta_{\lambda_7}^{(2)} = & +\frac{1}{8}g^4 [90\lambda_6 - 141\lambda_7] + \frac{1}{4}g^2g'^2 [10\lambda_6 + 29\lambda_7] + \frac{1}{8}g'^4 [30\lambda_6 + 187\lambda_7] + 20g_s^2\lambda_6 [3h_t^2 + h_b^2] \\
& +\frac{3}{8}g^2 [5\lambda_7(9h_t^2 + 3h_b^2 + h_\tau^2) - 288\lambda_7(\lambda_2 + \lambda_5) - 48\lambda_3(2\lambda_6 + \lambda_7) - 48\lambda_4(\lambda_6 + 2\lambda_7)] \\
& +\frac{1}{24}g'^2 [5\lambda_7(51h_t^2 + 5h_b^2 + 15h_\tau^2) - 48\lambda_6(6\lambda_3 + 4\lambda_4 - 2\lambda_5) \\
& \quad - 48\lambda_7(18\lambda_2 + 3\lambda_3 + 5\lambda_4 + 20\lambda_5)] \\
& -\frac{3}{4}\lambda_7 [11h_t^4 + 28h_t^2h_b^2 + 9h_b^4 + 3h_\tau^4]
\end{aligned}$$

$$\begin{aligned}
& + 6h_t^2\lambda_7[24\lambda_2 + 3\lambda_3 + 4\lambda_4 + 10\lambda_5] \\
& + (6h_b^2 + 2h_\tau^2)[\lambda_6(6\lambda_3 + 4\lambda_4 + 4\lambda_5) + \lambda_7(3\lambda_3 + 4\lambda_4 + 10\lambda_5)] \\
& - 6\lambda_7[-\lambda_1^2 + 53\lambda_2^2] - 4\lambda_1\lambda_7[9\lambda_3 + 7\lambda_4 + 10\lambda_5] - 4\lambda_2\lambda_7[33\lambda_3 + 35\lambda_4 + 74\lambda_5] \\
& - 2\lambda_7[16\lambda_3^2 + 34\lambda_3\lambda_4 + 72\lambda_3\lambda_5 + 17\lambda_4^2 + 76\lambda_4\lambda_5 + 72\lambda_5^2] \\
& - 4(\lambda_1 + \lambda_2)\lambda_6[9\lambda_3 + 7\lambda_4 + 10\lambda_5] \\
& - 2\lambda_6[18\lambda_3^2 + 28\lambda_3\lambda_4 + 40\lambda_3\lambda_5 + 17\lambda_4^2 + 44\lambda_4\lambda_5 + 84\lambda_5^2] \\
& - 3[14\lambda_6^3 + 11\lambda_6^2\lambda_7 + 42\lambda_6\lambda_7^2 + 37\lambda_7^3] . \tag{C.7}
\end{aligned}$$

In addition, the two-loop beta functions for the gauge and the supersymmetric Yukawa couplings may be listed as follows:

$$\beta_{g'}^{(2)} = \frac{5}{3}g'^3 \left( \frac{44}{5}g_s^2 + \frac{18}{5}g^2 + \frac{104}{15}g'^2 - \frac{17}{10}h_t^2 - \frac{1}{2}h_b^2 - \frac{3}{2}h_\tau^2 \right), \tag{C.8}$$

$$\beta_g^{(2)} = g^3 \left( 12g_s^2 + 8g^2 + 2g'^2 - \frac{3}{2}h_t^2 - \frac{3}{2}h_b^2 - \frac{1}{2}h_\tau^2 \right), \tag{C.9}$$

$$\beta_{g_s}^{(2)} = g_s^3 \left( -26g_s^2 + \frac{9}{2}g^2 + \frac{11}{6}g'^2 - 2h_t^2 - 2h_b^2 \right), \tag{C.10}$$

$$\begin{aligned}
\beta_{h_t}^{(2)} = & h_t \left[ -108g_s^4 + 9g_s^2g^2 + \frac{19}{9}g_s^2g'^2 - \frac{21}{4}g^4 - \frac{3}{4}g^2g'^2 + \frac{1267}{216}g'^4 \right. \\
& + g_s^2 \left( 36h_t^2 + \frac{16}{3}h_b^2 \right) + \frac{3}{16}g^2 \left( 75h_t^2 + 11h_b^2 \right) + \frac{1}{48}g'^2 \left( 393h_t^2 - \frac{41}{3}h_b^2 \right) \\
& - 12h_t^4 - \frac{5}{2}h_t^2h_b^2 - \frac{5}{2}h_b^4 - \frac{3}{4}h_b^2h_\tau^2 + 12h_t^2\lambda_2 + 2h_b^2(\lambda_3 - \lambda_4) \\
& \left. + 6\lambda_2^2 + \lambda_3^2 + \lambda_3\lambda_4 + \lambda_4^2 + 6\lambda_5^2 + \frac{3}{2}\lambda_6^2 + \frac{9}{2}\lambda_7^2 \right], \tag{C.11}
\end{aligned}$$

$$\begin{aligned}
\beta_{h_b}^{(2)} = & h_b \left[ -108g_s^4 + 9g_s^2g^2 + \frac{31}{9}g_s^2g'^2 - \frac{21}{4}g^4 - \frac{9}{4}g^2g'^2 + \frac{113}{216}g'^4 \right. \\
& + g_s^2 \left( \frac{16}{3}h_t^2 + 36h_b^2 \right) + \frac{3}{16}g^2 \left( 11h_t^2 + 75h_b^2 + 10h_\tau^2 \right) - \frac{1}{144}g'^2 \left( 53h_t^2 - 711h_b^2 - 450h_\tau^2 \right) \\
& - \frac{5}{2}h_t^4 - \frac{5}{2}h_t^2h_b^2 - 12h_b^4 - \frac{9}{4}h_b^2h_\tau^2 - \frac{9}{4}h_\tau^4 + 12h_b^2\lambda_1 + 2h_t^2(\lambda_3 - \lambda_4) \\
& \left. + 6\lambda_1^2 + \lambda_3^2 + \lambda_3\lambda_4 + \lambda_4^2 + 6\lambda_5^2 + \frac{9}{2}\lambda_6^2 + \frac{3}{2}\lambda_7^2 \right], \tag{C.12}
\end{aligned}$$

$$\begin{aligned}
\beta_{h_\tau}^{(2)} = & h_\tau \left[ 20g_s^2 h_b^2 - \frac{21}{4}g^4 + \frac{9}{4}g^2 g'^2 + \frac{161}{8}g'^4 \right. \\
& + \frac{15}{16}g^2 (6h_b^2 + 11h_\tau^2) + \frac{1}{48}g'^2 (50h_b^2 + 537h_\tau^2) \\
& - \frac{9}{4}h_t^2 h_b^2 - \frac{27}{4}h_b^4 - \frac{27}{4}h_b^2 h_\tau^2 - 3h_\tau^4 + 12h_\tau^2 \lambda_1 \\
& \left. + 6\lambda_1^2 + \lambda_3^2 + \lambda_3 \lambda_4 + \lambda_4^2 + 6\lambda_5^2 + \frac{9}{2}\lambda_6^2 + \frac{3}{2}\lambda_7^2 \right]. \tag{C.13}
\end{aligned}$$

Finally, the two-loop anomalous dimensions for the Higgs doublets are given by

$$\begin{aligned}
\gamma_1^{(2)} = & \frac{435}{32}g^4 - \frac{3}{16}g^2 g'^2 - \frac{149}{32}g'^4 - 20g_s^2 h_b^2 - \frac{15}{8}g^2 (3h_b^2 + h_\tau^2) - \frac{25}{24}g'^2 (h_b^2 + 3h_\tau^2) \\
& + \frac{9}{4}h_t^2 h_b^2 + \frac{27}{4}h_b^4 + \frac{9}{4}h_\tau^4 - 6\lambda_1^2 - \lambda_3^2 - \lambda_3 \lambda_4 - \lambda_4^2 - 6\lambda_5^2 - \frac{9}{2}\lambda_6^2 - \frac{3}{2}\lambda_7^2 \\
& - \frac{3}{2}t_\beta [2\lambda_1 \lambda_6 + 2\lambda_2 \lambda_7 + (\lambda_3 + \lambda_4 + 2\lambda_5)(\lambda_6 + \lambda_7)], \tag{C.14}
\end{aligned}$$

$$\begin{aligned}
\gamma_2^{(2)} = & \frac{435}{32}g^4 - \frac{3}{16}g^2 g'^2 - \frac{149}{32}g'^4 - h_t^2 (20g_s^2 + \frac{45}{8}g^2 + \frac{85}{24}g'^2) \\
& + \frac{27}{4}h_t^4 + \frac{9}{4}h_b^2 h_t^2 - 6\lambda_2^2 - \lambda_3^2 - \lambda_3 \lambda_4 - \lambda_4^2 - 6\lambda_5^2 - \frac{3}{2}\lambda_6^2 - \frac{9}{2}\lambda_7^2 \\
& - \frac{3}{2}t_\beta^{-1} [2\lambda_1 \lambda_6 + 2\lambda_2 \lambda_7 + (\lambda_3 + \lambda_4 + 2\lambda_5)(\lambda_6 + \lambda_7)]. \tag{C.15}
\end{aligned}$$

## D Threshold corrections to $\lambda_i$ at $M_S$

At the soft SUSY-breaking scale  $Q = M_S$ , we need to consider the threshold corrections to quartic couplings due to third-generation sfermions. These are derived in [33], which we extend here to include CP-violating phases.

The quartic couplings  $\lambda_i$  with  $i = 1 - 7$  at the RG scale  $Q = M_S$  are given by

$$\lambda_i(M_S) = \lambda_i^{(0)} + \sum_{n=1,2} \kappa^n \Delta^{(n)} \lambda_i, \tag{D.1}$$

where

$$\begin{aligned}
\lambda_1^{(0)} = \lambda_2^{(0)} = -\frac{1}{8}(g^2 + g'^2), \quad \lambda_3^{(0)} = -\frac{1}{4}(g^2 - g'^2), \quad \lambda_4^{(0)} = \frac{1}{2}g^2, \\
\lambda_5^{(0)} = \lambda_6^{(0)} = \lambda_7^{(0)} = 0, \tag{D.2}
\end{aligned}$$

and the one- and two-loop threshold corrections are <sup>||</sup>

$$\Delta^{(1)} \lambda_1 = \frac{1}{4}|h_t|^4 |\hat{\mu}|^4 - 3|h_b|^4 |\hat{A}_b|^2 \left( 1 - \frac{|\hat{A}_b|^2}{12} \right) - |h_\tau|^4 |\hat{A}_\tau|^2 \left( 1 - \frac{|\hat{A}_\tau|^2}{12} \right)$$

<sup>||</sup>Here all the mass parameters are dimensionless and normalized to the SUSY scale  $M_S$ :  $\hat{\mu} = \mu/M_S$ ,  $\hat{A}_{t,b,\tau} = A_{t,b,\tau}/M_S$ , and  $\hat{M}_3 = M_3/M_S$ .

$$\begin{aligned}
& -\frac{g^2 + g'^2}{8} (3|h_t|^2|\hat{\mu}|^2 - 3|h_b|^2|\hat{A}_b|^2 - |h_\tau|^2|\hat{A}_\tau|^2) \\
& + \frac{g^2 + g'^2}{24} (3|h_t|^2|\hat{\mu}|^2 + 3|h_b|^2|\hat{A}_b|^2 + |h_\tau|^2|\hat{A}_\tau|^2) , \tag{D.3}
\end{aligned}$$

$$\begin{aligned}
\Delta^{(1)}\lambda_2 = & -3|h_t|^4|\hat{A}_t|^2 \left( 1 - \frac{|\hat{A}_t|^2}{12} \right) + \frac{1}{4}|h_b|^4|\hat{\mu}|^4 + \frac{1}{12}|h_\tau|^4|\hat{\mu}|^4 \\
& + \frac{g^2 + g'^2}{8} (3|h_t|^2|\hat{A}_t|^2 - 3|h_b|^2|\hat{\mu}|^2 - |h_\tau|^2|\hat{\mu}|^2) \\
& + \frac{g^2 + g'^2}{24} (3|h_t|^2|\hat{A}_t|^2 + 3|h_b|^2|\hat{\mu}|^2 + |h_\tau|^2|\hat{\mu}|^2) , \tag{D.4}
\end{aligned}$$

$$\begin{aligned}
\Delta^{(1)}\lambda_3 = & -\frac{1}{6}|\mu|^2 [3|h_t|^4(3 - |\hat{A}_t|^2) + 3|h_b|^4(3 - |\hat{A}_b|^2) + |h_\tau|^4(3 - |\hat{A}_\tau|^2)] \\
& - \frac{1}{2}|h_t|^2|h_b|^2 [3|\hat{A}_t + \hat{A}_b|^2 - ||\hat{\mu}|^2 - \hat{A}_t \hat{A}_b^*|^2 - 6|\hat{\mu}|^2] \\
& + \frac{g^2 - g'^2}{8} [3|h_t|^2(|\hat{A}_t|^2 - |\hat{\mu}|^2) + 3|h_b|^2(|\hat{A}_b|^2 - |\hat{\mu}|^2) + |h_\tau|^2(|\hat{A}_\tau|^2 - |\hat{\mu}|^2)] \\
& + \frac{g^2 - g'^2}{24} [3|h_t|^2(|\hat{A}_t|^2 + |\hat{\mu}|^2) + 3|h_b|^2(|\hat{A}_b|^2 + |\hat{\mu}|^2) + |h_\tau|^2(|\hat{A}_\tau|^2 + |\hat{\mu}|^2)] , \tag{D.5}
\end{aligned}$$

$$\begin{aligned}
\Delta^{(1)}\lambda_4 = & -\frac{1}{6}|\mu|^2 [3|h_t|^4(3 - |\hat{A}_t|^2) + 3|h_b|^4(3 - |\hat{A}_b|^2) + |h_\tau|^4(3 - |\hat{A}_\tau|^2)] \\
& + \frac{1}{2}|h_t|^2|h_b|^2 [3|\hat{A}_t + \hat{A}_b|^2 - ||\hat{\mu}|^2 - \hat{A}_t \hat{A}_b^*|^2 - 6|\hat{\mu}|^2] \\
& - \frac{g^2}{4} [3|h_t|^2(|\hat{A}_t|^2 - |\hat{\mu}|^2) + 3|h_b|^2(|\hat{A}_b|^2 - |\hat{\mu}|^2) + |h_\tau|^2(|\hat{A}_\tau|^2 - |\hat{\mu}|^2)] \\
& - \frac{g^2}{12} [3|h_t|^2(|\hat{A}_t|^2 + |\hat{\mu}|^2) + 3|h_b|^2(|\hat{A}_b|^2 + |\hat{\mu}|^2) + |h_\tau|^2(|\hat{A}_\tau|^2 + |\hat{\mu}|^2)] , \tag{D.6}
\end{aligned}$$

$$\Delta^{(1)}\lambda_5 = \frac{1}{12} [3h_t^4\hat{\mu}^2\hat{A}_t^2 + 3h_b^4\hat{\mu}^2\hat{A}_b^2 + h_\tau^4\hat{\mu}^2\hat{A}_\tau^2] , \tag{D.7}$$

$$\Delta^{(1)}\lambda_6 = -\frac{1}{6} [3h_t^4|\hat{\mu}|^2\hat{\mu}\hat{A}_t + 3h_b^4\hat{\mu}\hat{A}_b(|\hat{A}_b|^2 - 6) + h_\tau^4\hat{\mu}\hat{A}_\tau(|\hat{A}_\tau|^2 - 6)] , \tag{D.8}$$

$$\Delta^{(1)}\lambda_7 = -\frac{1}{6} [3h_t^4\hat{\mu}\hat{A}_t(|\hat{A}_t|^2 - 6) + 3h_b^4|\hat{\mu}|^2\hat{\mu}\hat{A}_b + h_\tau^4|\hat{\mu}|^2\hat{\mu}\hat{A}_\tau] , \tag{D.9}$$

where  $h_{t,b,\tau} = h_{t,b,\tau}^{\text{MSSM}}$  at the RG scale  $Q = M_S$ .

The two-loop corrections of  $\mathcal{O}(|h_t|^4 g_s^2)$  are given by

$$\Delta^{(2)}\lambda_1 = \frac{2}{3}|h_t|^4 g_s^2 |\hat{\mu}|^4 , \tag{D.10}$$

$$\Delta^{(2)}\lambda_2 = -8|h_t|^4 g_s^2 \left[ -2\Re(\hat{A}_t \hat{M}_3^*) + \frac{1}{3}|\hat{A}_t|^2 \Re(\hat{A}_t \hat{M}_3^*) - \frac{1}{12}|\hat{A}_t|^4 \right] , \tag{D.11}$$

$$\Delta^{(2)}\lambda_3 = \Delta^{(2)}\lambda_4 = -\frac{4}{3}|h_t|^4 g_s^2 |\hat{\mu}|^2 \left[ \operatorname{Re}(\hat{A}_t \hat{M}_3^*) - \frac{1}{2} |\hat{A}_t|^2 \right], \quad (\text{D.12})$$

$$\Delta^{(2)}\lambda_5 = -\frac{2}{3}|h_t|^4 g_s^2 \hat{\mu} \hat{A}_t \left[ \hat{\mu} \hat{M}_3 - \frac{1}{2} \hat{\mu} \hat{A}_t \right], \quad (\text{D.13})$$

$$\Delta^{(2)}\lambda_6 = -\frac{4}{3}|h_t|^4 g_s^2 |\hat{\mu}|^2 \left[ -\hat{\mu} \hat{M}_3 + \hat{\mu} \hat{A}_t \right], \quad (\text{D.14})$$

$$\Delta^{(2)}\lambda_7 = -4|h_t|^4 g_s^2 \left[ 2\hat{\mu} \hat{M}_3 - \frac{1}{3} \hat{\mu} \hat{A}_t^2 \hat{M}_3^* - \frac{2}{3} |\hat{A}_t|^2 \hat{\mu} \hat{M}_3 + \frac{1}{3} |\hat{A}_t|^2 \hat{\mu} \hat{A}_t \right]. \quad (\text{D.15})$$

## References

- [1] See, for example, J. R. Ellis and D. Ross, “A Light Higgs boson would invite supersymmetry,” *Phys. Lett. B* **506** (2001) 331 [hep-ph/0012067].
- [2] J. R. Ellis, G. Ridolfi and F. Zwirner, “Radiative corrections to the masses of supersymmetric Higgs bosons,” *Phys. Lett. B* **257** (1991) 83.
- [3] H. E. Haber and R. Hempfling, “Can the mass of the lightest Higgs boson of the minimal supersymmetric model be larger than  $m(Z)$ ?” *Phys. Rev. Lett.* **66** (1991) 1815.
- [4] Y. Okada, M. Yamaguchi and T. Yanagida, “Upper bound of the lightest Higgs boson mass in the minimal supersymmetric standard model,” *Prog. Theor. Phys.* **85** (1991) 1.
- [5] G. Aad *et al.* [ATLAS and CMS Collaborations], “Combined Measurement of the Higgs Boson Mass in  $pp$  Collisions at  $\sqrt{s} = 7$  and 8 TeV with the ATLAS and CMS Experiments,” *Phys. Rev. Lett.* **114** (2015) 191803 [arXiv:1503.07589 [hep-ex]].
- [6] See, for example, J. R. Ellis, S. Heinemeyer, K. A. Olive and G. Weiglein, “Precision analysis of the lightest MSSM Higgs boson at future colliders,” *JHEP* **0301** (2003) 006 [hep-ph/0211206].
- [7] ATLAS and CMS Collaborations, “Measurements of the Higgs boson production and decay rates and constraints on its couplings from a combined ATLAS and CMS analysis of the LHC  $pp$  collision data at  $\sqrt{s} = 7$  and 8 TeV,” ATLAS-CONF-2015-044, CMS-PAS-HIG-15-002,  
<https://cds.cern.ch/record/2052552/files/ATLAS-CONF-2015-044.pdf>.
- [8] M. Carena, J. R. Ellis, A. Pilaftsis and C. E. M. Wagner, “CP violating MSSM Higgs bosons in the light of LEP-2,” *Phys. Lett. B* **495** (2000) 155 [hep-ph/0009212].
- [9] A. Pilaftsis, “CP odd tadpole renormalization of Higgs scalar - pseudoscalar mixing,” *Phys. Rev. D* **58** (1998) 096010 [hep-ph/9803297].
- [10] A. Pilaftsis, “Higgs scalar - pseudoscalar mixing in the minimal supersymmetric standard model,” *Phys. Lett. B* **435** (1998) 88 [hep-ph/9805373].
- [11] A. Pilaftsis and C. E. M. Wagner, “Higgs bosons in the minimal supersymmetric standard model with explicit CP violation,” *Nucl. Phys. B* **553** (1999) 3 [hep-ph/9902371].
- [12] D. A. Demir, “Effects of the supersymmetric phases on the neutral Higgs sector,” *Phys. Rev. D* **60** (1999) 055006 [hep-ph/9901389].
- [13] S. Y. Choi, M. Drees and J. S. Lee, “Loop corrections to the neutral Higgs boson sector of the MSSM with explicit CP violation,” *Phys. Lett. B* **481** (2000) 57 [hep-ph/0002287].
- [14] M. S. Carena, J. R. Ellis, A. Pilaftsis and C. E. M. Wagner, “Renormalization group improved effective potential for the MSSM Higgs sector with explicit CP violation,” *Nucl. Phys. B* **586** (2000) 92 [hep-ph/0003180].

- [15] T. Ibrahim and P. Nath, “Corrections to the Higgs boson masses and mixings from chargino, W and charged Higgs exchange loops and large CP phases,” *Phys. Rev. D* **63** (2001) 035009 [hep-ph/0008237].
- [16] M. S. Carena, J. R. Ellis, A. Pilaftsis and C. E. M. Wagner, “Higgs boson pole masses in the MSSM with explicit CP violation,” *Nucl. Phys. B* **625** (2002) 345 [hep-ph/0111245].
- [17] T. Ibrahim and P. Nath, “Neutralino exchange corrections to the Higgs boson mixings with explicit CP violation,” *Phys. Rev. D* **66** (2002) 015005 [hep-ph/0204092].
- [18] J. R. Ellis, J. S. Lee and A. Pilaftsis, *JHEP* **0810** (2008) 049 [arXiv:0808.1819 [hep-ph]].
- [19] T. Ibrahim and P. Nath, “The Neutron and the lepton EDMs in MSSM, large CP violating phases, and the cancellation mechanism,” *Phys. Rev. D* **58** (1998) 111301 [*Phys. Rev. D* **60** (1999) 099902] [hep-ph/9807501].
- [20] M. Brhlik, G. J. Good and G. L. Kane, “Electric dipole moments do not require the CP violating phases of supersymmetry to be small,” *Phys. Rev. D* **59** (1999) 115004 [hep-ph/9810457].
- [21] J. Ellis, J. S. Lee and A. Pilaftsis, “A Geometric Approach to CP Violation: Applications to the MCPMFV SUSY Model,” *JHEP* **1010** (2010) 049 [arXiv:1006.3087 [hep-ph]].
- [22] N. Yamanaka, T. Sato and T. Kubota, “Linear programming analysis of the  $R$ -parity violation within EDM-constraints,” *JHEP* **1412** (2014) 110 [arXiv:1406.3713 [hep-ph]].
- [23] B. Li and C. E. M. Wagner, “CP-odd component of the lightest neutral Higgs boson in the MSSM,” *Phys. Rev. D* **91**, 095019 (2015) [arXiv:1502.02210 [hep-ph]].
- [24] J. R. Ellis, J. S. Lee and A. Pilaftsis, “B-Meson Observables in the Maximally CP-Violating MSSM with Minimal Flavour Violation,” *Phys. Rev. D* **76** (2007) 115011 [arXiv:0708.2079 [hep-ph]].
- [25] A. Arbey, J. Ellis, R. M. Godbole and F. Mahmoudi, *Eur. Phys. J. C* **75**, no. 2, 85 (2015) [arXiv:1410.4824 [hep-ph]].
- [26] J. S. Lee, A. Pilaftsis, M. S. Carena, S. Y. Choi, M. Drees, J. R. Ellis and C. E. M. Wagner, “CPsuperH: A Computational tool for Higgs phenomenology in the minimal supersymmetric standard model with explicit CP violation,” *Comput. Phys. Commun.* **156** (2004) 283 [hep-ph/0307377].
- [27] J. S. Lee, M. Carena, J. Ellis, A. Pilaftsis and C. E. M. Wagner, “CPsuperH2.0: an Improved Computational Tool for Higgs Phenomenology in the MSSM with Explicit CP Violation,” *Comput. Phys. Commun.* **180** (2009) 312 [arXiv:0712.2360 [hep-ph]].
- [28] J. S. Lee, M. Carena, J. Ellis, A. Pilaftsis and C. E. M. Wagner, “CPsuperH2.3: an Updated Tool for Phenomenology in the MSSM with Explicit CP Violation,” *Comput. Phys. Commun.* **184** (2013) 1220 [arXiv:1208.2212 [hep-ph]].

- [29] S. Heinemeyer, W. Hollik, H. Rzehak and G. Weiglein, “The Higgs sector of the complex MSSM at two-loop order: QCD contributions,” *Phys. Lett. B* **652** (2007) 300 [arXiv:0705.0746 [hep-ph]]; <http://www.feynhiggs.de>.
- [30] T. Hahn, S. Heinemeyer, W. Hollik, H. Rzehak and G. Weiglein, “High-Precision Predictions for the Light CP-Even Higgs Boson Mass of the Minimal Supersymmetric Standard Model,” *Phys. Rev. Lett.* **112** (2014) 14, 141801 [arXiv:1312.4937 [hep-ph]].
- [31] H. E. Haber and R. Hempfling, “The Renormalization group improved Higgs sector of the minimal supersymmetric model,” *Phys. Rev. D* **48** (1993) 4280 [hep-ph/9307201].
- [32] P. S. B. Dev and A. Pilaftsis, “Maximally Symmetric Two Higgs Doublet Model with Natural Standard Model Alignment,” *JHEP* **1412** (2014) 024 [arXiv:1408.3405 [hep-ph]].
- [33] G. Lee and C. E. M. Wagner, “Higgs Bosons in Heavy Supersymmetry with an Intermediate  $m_A$ ,” arXiv:1508.00576 [hep-ph].
- [34] J. Guasch, W. Hollik and S. Penaranda, “Distinguishing Higgs models in  $H \rightarrow b \bar{b}$  /  $H \rightarrow \tau^+ \tau^-$ ,” *Phys. Lett. B* **515** (2001) 367 [hep-ph/0106027].
- [35] P. Draper, G. Lee and C. E. M. Wagner, “Precise Estimates of the Higgs Mass in Heavy SUSY,” *Phys. Rev. D* **89** (2014) 055023 [arXiv:1312.5743 [hep-ph]].
- [36] D. Buttazzo, G. Degrassi, P. P. Giardino, G. F. Giudice, F. Sala, A. Salvio and A. Strumia, “Investigating the near-criticality of the Higgs boson,” *JHEP* **1312**, 089 (2013) [arXiv:1307.3536 [hep-ph]].
- [37] K. Melnikov and T. v. Ritbergen, “The Three loop relation between the MS-bar and the pole quark masses,” *Phys. Lett. B* **482** (2000) 99 [hep-ph/9912391].
- [38] M. Carena, S. Heinemeyer, C. E. M. Wagner and G. Weiglein, “Suggestions for benchmark scenarios for MSSM Higgs boson searches at hadron colliders,” *Eur. Phys. J. C* **26** (2003) 601 [hep-ph/0202167].
- [39] M. Carena, S. Heinemeyer, O. Stal, C. E. M. Wagner and G. Weiglein, “MSSM Higgs Boson Searches at the LHC: Benchmark Scenarios after the Discovery of a Higgs-like Particle,” *Eur. Phys. J. C* **73** (2013) 9, 2552 [arXiv:1302.7033 [hep-ph]].
- [40] J. R. Ellis, J. S. Lee and A. Pilaftsis, “CERN LHC signatures of resonant CP violation in a minimal supersymmetric Higgs sector,” *Phys. Rev. D* **70** (2004) 075010 doi:10.1103/PhysRevD.70.075010 [hep-ph/0404167].
- [41] S. Berge, W. Bernreuther and S. Kirchner, “Prospects of constraining the Higgs CP nature in the tau decay channel at the LHC,” arXiv:1510.03850 [hep-ph].
- [42] H. Arason, D. J. Castano, B. Keszthelyi, S. Mikaelian, E. J. Piard, P. Ramond and B. D. Wright, “Renormalization group study of the standard model and its extensions. 1. The Standard model,” *Phys. Rev. D* **46** (1992) 3945.